Upregulation of inward rectifier K$^+$ (Kir2) channels in dentate gyrus granule cells in temporal lobe epilepsy

Christina C. Young[1,2], Michael Stegen[1,3], René Bernard[4], Martin Müller[3,5], Josef Bischofberger[6], Rüdiger W. Veh[4], Carola A. Haas[5] and Jakob Wolfart[1]

[1]*Cellular Neurophysiology, Dept. of Neurosurgery, University Medical Center Freiburg, Breisacher Str. 64, 79106 Freiburg, Germany*
[2]*Faculty of Biology, University of Freiburg, Schaenzlestrasse 1, 79104 Freiburg, Germany*
[3]*Faculty of Pharmaceutical Sciences, University of Freiburg, Hebelstraße 27, 79085 Freiburg, Germany*
[4]*Institut für Integrative Neuroanatomie, Charité – Universitätsmedizin Berlin, Philippstr. 12, 10115 Berlin, Germany*
[5]*Experimental Epilepsy Research Group, Dept. of Neurosurgery, University Medical Center Freiburg, Breisacher Str. 64, 79106 Freiburg, Germany*
[6]*Physiological Institute, University of Freiburg, Hermann-Herder-Straße 7, 79104 Freiburg, Germany*

In humans, temporal lobe epilepsy (TLE) is often associated with Ammon's horn sclerosis (AHS) characterized by hippocampal cell death, gliosis and granule cell dispersion (GCD) in the dentate gyrus. Granule cells surviving TLE have been proposed to be hyperexcitable and to play an important role in seizure generation. However, it is unclear whether this applies to conditions of AHS. We studied granule cells using the intrahippocampal kainate injection mouse model of TLE, brain slice patch-clamp recordings, morphological reconstructions and immunocytochemistry. With progressing AHS and GCD, 'epileptic' granule cells of the injected hippocampus displayed a decreased input resistance, a decreased membrane time constant and an increased rheobase. The resting leak conductance was doubled in epileptic granule cells and roughly 70–80% of this difference were sensitive to K$^+$ replacement. Of the increased K$^+$ leak, about 50% were sensitive to 1 mM Ba^{2+}. Approximately 20–30% of the pathological leak was mediated by a bicuculline-sensitive GABA$_A$ conductance. Epileptic granule cells had strongly enlarged inwardly rectifying currents with a low micromolar Ba^{2+} IC$_{50}$, reminiscent of classic inward rectifier K$^+$ channels (Irk/Kir2). Indeed, protein expression of Kir2 subunits (Kir2.1, Kir2.2, Kir2.3, Kir2.4) was upregulated in epileptic granule cells. Immunolabelling for two-pore weak inward rectifier K$^+$ channels (Twik1/K2P1.1, Twik2/K2P6.1) was also increased. We conclude that the excitability of granule cells in the sclerotic focus of TLE is reduced due to an increased resting conductance mainly due to upregulated K$^+$ channel expression. These results point to a local adaptive mechanism that could counterbalance hyperexcitability in epilepsy.

Abbreviations AHS, Ammon's horn sclerosis; GCD, granule cell dispersion; g_{rest}, resting leak conductance; KA, kainic acid; K2P/Twik, two-pore weak inward rectifier K$^+$; Kir2/Irk, classic inward rectifier K$^+$; Kir3/Girk, G-protein-coupled inward rectifier K$^+$; R_{in}, input resistance; R_m, specific membrane resistance; τ_m, membrane time constant; TLE, mesial temporal lobe epilepsy; V_{rest}, resting membrane potential

Mesial temporal lobe epilepsy (TLE), one of the most prevalent forms of focal epilepsies, is often intractable but surgical resection of the hippocampus and adjacent medial temporal structures leads to seizure cessation in most cases. Resected hippocampi of TLE patients often show Ammon's horn sclerosis (AHS), characterized by marked hippocampal cell death, gliosis and network

disorganization (Blumcke *et al.* 2002; Thom *et al.* 2002). Closely linked to hippocampal damage is granule cell dispersion (GCD) in the dentate gyrus (Houser, 1990; Thom *et al.* 2002).

The role of granule cells in TLE is not clear. Granule cells survive hippocampal damage better than neighbouring cell populations and have been implicated in seizure generation (Sloviter, 1991; Heinemann *et al.* 1992; Okazaki *et al.* 1999; Selke *et al.* 2006). On the other hand, doubts have been raised whether granule cells actively contribute

---

Christina C. Young and Michael Stegen contributed equally to this work.

to seizures (Sloviter, 1994; Liu *et al.* 2000; Harvey & Sloviter, 2005). Furthermore, although the structural changes in AHS are often considered a 'pathological substrate' for TLE (Blumcke *et al.* 2002; Thom *et al.* 2002), it is unclear whether the sclerotic tissue really is the origin of hyperexcitability in TLE (King *et al.* 1997; Mueller *et al.* 2007; Le Duigou *et al.* 2008). In particular, only little is known about the electrophysiology of granule cells in relation to AHS and GCD.

Recently, we found a reduced input resistance (R_{in}) and an increased inwardly rectifying conductance in granule cells of TLE patients with AHS (Stegen *et al.* 2009), a result which contrasted with a large number of previous results on intrinsic properties of granule cells in TLE patients and TLE animal models (e.g. Mody *et al.* 1988, 1992; Williamson *et al.* 1995; Isokawa, 1996*b*; Molnar & Nadler, 1999; Okazaki *et al.* 1999; Scharfman *et al.* 2000; Dietrich *et al.* 2005; Selke *et al.* 2006). To further study the underlying mechanisms under controlled conditions, we utilized the focal KA injection mouse model of TLE where not only recurrent, focal, pharmaco-resistant seizures but also AHS and GCD have been well characterized (Suzuki *et al.* 1995; Bouilleret *et al.* 1999; Riban *et al.* 2002; Kralic *et al.* 2005; Le Duigou *et al.* 2005; Heinrich *et al.* 2006). Using patch-clamp recordings of granule cells in brain slices, we found an increased resting conductance with progressing AHS. In addition, we used quantitative pharmacology, quantitative morphology, computer simulations and immunocytochemistry to identify mechanisms responsible for the increased leak conductance. Our results suggest that the increased leak was due to an upregulation of inward rectifier K^+ (Kir) channels, in particular of the Kir2 type, in combination with an increased $GABA_A$ conductance. These results point to homeostatic mechanisms in TLE that could result in shunting of epileptic input and thereby protect granule cells in the sclerotic focus.

Methods

Animals

All animal procedures were performed in accordance with the guidelines of the European Community Council Directive of November 24, 1986 (86/609/EEC) and were approved by the regional council and local animal welfare officer according to the German animal protection act (Tierschutzgesetz). Experiments were conducted on male C57Bl/6 mice (64 controls, 119 KA injections, 3 saline injections and 3 mice for immunocytochemistry). Animals were held in a 12 h light–dark cycle (room temperature, 21.5–22.5°C) with food and water *ad libitum*. Before decapitation and brain removal mice were anaesthetized with isofluorane.

KA injections

Kainic acid (KA, in 0.9% NaCl) or saline injections were performed as previously described (Heinrich *et al.* 2006). Briefly, 5- to 6-week-old mice were anaesthetized I.P. with a mixture of (in μg (g body weight)$^{-1}$) 100 ketamine, 5 xylazin and 0.1 atropin and placed into a stereotaxic frame. Fifty nanolitres of a 20 mM KA solution in 0.9% NaCl were injected into the right dorsal CA1 region of the hippocampus during 1 min using a 0.5 μl microsyringe (Hamilton, Bonaduz, Switzerland) and a micropump (CMA/100, Carnegie Medicine, Stockholm, Sweden). The coordinates for injection (with bregma as reference) were: anteroposterior 1.9 mm, mediolateral 1.5 mm and dorsoventral 1.9 mm. The cannula was left two additional minutes after injection to avoid reflux along the cannula track. After recovery from anaesthesia a status epilepticus of several hours was observed. Since, in this model morphological, electrophysiological and behavioural symptoms of chronic TLE develop within 2 weeks post-KA injection (Suzuki *et al.* 1995; Bouilleret *et al.* 1999; Heinrich *et al.* 2006), experiments were performed 2–8 weeks after KA injection, if not stated otherwise.

Brain slice preparation

Mice (6 to 15 weeks old; control 6–11 weeks, KA-injected 6–15 weeks) were deeply anaesthetized with isoflurane and killed by decapitation. The brain was immersed in ice-cold artificial cerebrospinal fluid (ACSF) containing (in mM): 87 NaCl, 25 NaHCO$_3$, 2.5 KCl, 1.25 NaH$_2$PO$_4$, 0.5 CaCl$_2$, 7 MgCl$_2$, 75 sucrose and 10 glucose (equilibrated with 95% O$_2$–5% CO$_2$). Coronal slices 400 μm thick were collected with a vibratome VT1200S (Leica, Bensheim, Germany) from the dorsal hippocampus (in KA-injected mice approximately ±0.8 mm from the injection site). Slices were incubated for 30 min at 35–36°C and subsequently kept at room temperature in oxygenated sucrose ACSF for more than 1 h until they were transferred individually for electrophysiological experiments.

Electrophysiology

Patch-clamp methods were adopted from (Schmidt-Hieber *et al.* 2004, 2007). For patch-clamp recordings, brain slices were transferred to a recording chamber and continuously superfused at room temperature with ACSF containing (in mM): 125 NaCl, 25 NaHCO$_3$, 2.5 KCl, 1.25 NaH$_2$PO$_4$, 2 CaCl$_2$, 1 MgCl$_2$ and 25 glucose (equilibrated with 95% O$_2$–5% CO$_2$). Recordings were obtained from neurons in the upper blade of the dentate gyrus granule cell layer visualized by differential interference contrast video microscopy using

a 63×/1.0 objective in an upright microscope (Axioskop2 FS, Zeiss, Oberkochen, Germany). Cells of KA-injected animals were from the injected side ('epileptic') or the un-injected side (contralateral) or from naive animals ('control'). To exclude new-born neurons from the analysis we avoided recording at the border between granule cell layer and hilus (Schmidt-Hieber *et al.* 2004). Patch pipettes were pulled from borosilicate glass using a DMZ-universal puller (Zeitz, Martinsried, Germany). They were filled with a solution containing (in mM): 135 potassium gluconate, 20 KCl, 10 Hepes, 0.1 EGTA, 2 MgCl$_2$, 2 Na$_2$ATP and 0.2% biocytin (pH = 7.28) and had tip resistances of 5.2 ± 0.04 MΩ (range 3.3–7.7). To obtain optimal biocytin labelling, the whole-cell configuration was maintained for at least 25 min and the pipette was retrieved via the outside-out configuration. Records were filtered at 8–10 kHz using a SEC05LX amplifier (NPI, Tamm, Germany) and digitized at 10–20 kHz (voltage and current clamp, respectively) using a ITC18 D/A converter (Instrutech, Port Washington, NY, USA) and PatchMaster software (Heka, Lambrecht, Germany). Series resistances (7–16 MΩ) were compensated via bridge balance and pipette capacitance was compensated via fast capacitance controls of the SEC amplifier. Seal resistances (R_{seal}) were >1 GΩ (control, 3.3 ± 0.2 GΩ, $n = 125$; epileptic, 2.5 ± 0.1 GΩ, $n = 197$, $P < 0.001$). Accepted ratios of $R_{\text{in}}/R_{\text{seal}}$ were less than 0.3 (control, 0.15 ± 0.01, $n = 125$; epileptic, 0.11 ± 0.004, $n = 197$, $P < 0.001$), except when stated otherwise (<0.1). The liquid junction potential was determined to be 10 mV and voltages were appropriately corrected (Staley & Mody, 1992; Okazaki *et al.* 1999). Only cells with resting membrane potentials (V_{rest}) negative to -65 mV and overshooting action potentials were included in the analysis.

Pharmacology

In K$^+$ replacement experiments cells were first recorded with normal intracellular solution and (via the outside out configuration) subsequently repatched with K$^+$-free intracellular solution. In these cases, K$^+$ was replaced equimolar with TEA in the ACSF and the pipette solution contained (in mM): 135 TEACl, 20 CsCl, 0.1 EGTA, 2 MgCl$_2$, 2 Na$_2$ATP and 0.2% biocytin (pH 7.28 adjusted with TEA hydroxide). Except in current-clamp conditions, experiments were conducted in the presence of the Na$^+$ channel blocker tetrodotoxin (TTX, 0.5 μM) and inhibitors of AMPA/KA-type and NMDA-type glutamate receptors using 50 μM D(-)-2-amino-5-phosphonopentanoic acid (D-AP5) and 20 μM 1,2,3,4-tetrahydro-7-nitro-2,3-dioxoquinoxaline-6-carbonitrile disodium (CNQX) as mentioned in the text. The following drugs were kept in H$_2$O stocks at -20°C: 1(S),9(R)-(−)-bicuculline

methiodide (BMI), bupivacaine-HCl, CsCl, CNQX, D-AP5, TEACL, TTX, BaCl$_2$, 4-aminopyridine (4-AP), 1,3-dihydro-1-phenyl-3,3-bis(4-pyridinylmethyl)-2H-indol-2-one (linopirdine), apamin, r-tertiapinQ, 10,10-bis(4-pyridinylmethyl)-9(10H)-anthracenone dihydrochloride (XE991), 4-ethylphenylamino-1,2-dimethyl-6-methylaminopyrimidinium chloride (ZD7288). PTX and tolbutamide were kept in DMSO stocks at -20°C and diluted (1 : 1000) freshly in oxygenated glucose ACSF. (RS)-3-amino-2-(4-chlorophenyl)propylphosphonic acid (phaclofen) was solved in 100 mM NaOH. Drugs were kept in glass syringes of an application system (Auto-Mate Scientific, Berkeley, CA, USA) under carbogen pressurized at 1300–1600 hPa before bath application. We obtained D-AP5, CNQX, XE991 and ZD7288 from Ascent Scientific (Weston-Super-Mare, UK), apamin and linopirdine from Tocris (Bristol, UK), r-tertiapin-Q from Alomone (Jerusalem, Israel), tolbutamide from ICN Biomedicals (Aurora, OH, USA) and all other substances from Sigma-Aldrich (Taufkirchen, Germany).

Morphology and immunocytochemistry

For cell type identification, slices were fixed overnight with 4% paraformaldehyde in 0.1 M PB pH 7.4. After 3 washing steps with PB, slices were treated for 30 min with a blocking solution containing 0.3% Triton X-100 and 10% normal goat serum (NGS) and incubated either for more than 3 h at room temperature or overnight at 4°C with a rabbit polyclonal anti-Prox1 antibody, (1 : 1000, Chemicon, Temecula, CA, USA) in 0.1% Triton and 1% NGS. After 3 washes, slices were incubated with Alexa Fluor-546-streptavidin (1 : 500, Invitrogen, Karlsruhe, Germany) for biotin detection and a secondary anti-rabbit antibody conjugated with Alexa Fluor-488 (1 : 200, Invitrogen) either for more than 3 h at room temperature or overnight at 4°C. After 5 washes, slices were mounted in fluorescence mounting medium (DAKO, Glastrup, Denmark) or ProLong gold antifade reagent (Invitrogen). For overview reconstructions, GCD measurements and cell identification immunofluorescence was analysed with an Axioplan 2 microscope equipped with Apotome technology (Zeiss) using the 20×/0.75 objective and extended focal images. GCD was quantified as width of granule cell layer measured at the position and level of reconstructed neurons. If a recorded cell could not unambiguously be identified by biocytin staining, three GCD measurements per slice were averaged. The experimenters performing the GCD measurements were unaware of the respective electrophysiological results.

For detailed reconstructions using confocal microscopy, slices were washed 4 times after fixation and were incubated with FITC–AvidinD (1 : 500, Vector

Laboratories, Burlingame, CA, USA) in 0.3% Triton (in 0.1 M PB) overnight at 4°C. After 3 washes, slices were mounted in ProLong gold antifade reagent (Invitrogen) and stored 7 days prior to confocal acquisition. For detailed morphological reconstructions of cellular compartments, we used a Zeiss LSM 510 equipped with an argon laser (488 nm), a long-pass emission filter (LP505) and a 40×/1.3 NA oil-immersion objective. Soma, axon and dendrites were traced using image stacks ($0.25 \times 0.25 \, \mu$m pixel^{-1} to $0.32 \times 0.32 \, \mu$m pixel^{-1} in x–y plane, $0.5 \, \mu$m in z-axis) with the filament tracing software Neurolucida (mbf Bioscience, Williston, VT, USA). Spines were manually counted with variably sized markers and spine surface was estimated by assuming sphere-like shapes neglecting spine necks. We did not correct for hidden spines and for tissue shrinkage.

For Kir channel and Twik channel immunoperoxidase cytochemistry, animals were deeply anaesthetized by intraperitoneal injections of a cocktail consisting of 45% ketamine (100 mg ml^{-1}), 35% xylazine (20 mg ml^{-1}) and 20% saline, at a dose of 0.16 ml (100 g of body weight)$^{-1}$. After 200 IU heparin I.P. they were fixed via transcardial perfusion with 4% paraformaldehyde, 0.05% glutaraldehyde and 0.2% picric acid in 0.1 M PB, pH 7.4 (PGPic). Brains were removed from the skull, cut into preselected blocks, cryoprotected in 0.4 M sucrose for about 4 h and in 0.8 M sucrose overnight, shock-frozen in hexane at −70°C, and stored at −80°C until use. Coronal 20-μm-thick cryostat sections were stored at −20°C in a cryoprotectant solution (30% sucrose and 30% ethylene glycol in 0.1 M PB, pH 7.4) until use. Freely floating sections were rinsed in 0.01 M PBS at pH 7.4, treated for 15 min with 1% sodium borohydride in PBS and thoroughly washed in PBS. Thereafter, sections were pretreated for 30 min in a blocking and permeabilizing solution, consisting of 10% NGS (Interchem, Bad Kreuznach, Germany), 0.3% Triton X-100 and 0.05% phenylhydrazine (Merck, Darmstadt, Germany) in PBS at RT. Primary antibodies against Kir2 and Kir3 channels (Pruss *et al.* 2003; Eulitz *et al.* 2007) or against Twik channels were diluted (Kir2.1, 1 : 500; Kir2.2; 1 : 100; Kir2.3, 1 : 100; Kir2.4, 1 : 5000; Kir3.1, 1 : 5000; Kir3.2, 1 : 1000; Kir3.3, 1 : 5000; Kir3.4, 1 : 100; Twik1, 1 : 200, sc-11483, Santa Cruz, Santa Cruz, CA, USA; Twik, 1 : 500, APC-040, Alomone Labs) in PBS containing 10% NGS, 0.3% Triton X-100, 0.1% sodium azide and 0.01% thiomersal, and applied for 36 h at 2°C. Thereafter, sections were thoroughly rinsed in PBS, pretreated for 1 h with 0.2% bovine serum albumin in PBS (PBS-A), and exposed for another 24 h to the secondary antibodies (biotinylated goat anti-rabbit IgG, 1 : 2000; biotinylated horse anti-goat IgG, 1 : 2000; both from Vector Labs). After repeated washings in PBS and preincubation for 1 h in PBS-A, the biotinylated secondary antibodies in the sections were complexed for

another 12 h with a preformed ABC-complex (Vector Labs, 1 : 200 in PBS-A). After further thorough rinses in PBS, preincubation for 15 min in a solution of 0.05% diaminobenzidine and 10 mM imidazole in 50 mM Tris buffer, pH 7.6, the visualization of the antigen–antibody complexes was started by the addition of hydrogen peroxide (0.0015%; 25 μl of 0.03% hydrogen peroxide to 500 μl solution) and stopped after 15 min at RT by repeated washings with PBS. Sections were mounted onto gelatin-coated slides, air-dried, dehydrated through a graded series of ethanol, transferred to xylene, and coverslipped with Entellan (Merck). For cresyl violet staining slide-mounted sections were left in 70% ethanol overnight, rinsed in bidistilled water, and stained with 0.2% cresyl violet acetate in 20 mM acetate buffer, pH 4.0, for 30 min at RT. After rinsing in bidistilled water, sections were dehydrated and coverslipped.

Cable modelling

Passive cable models were obtained using NEURON 6.2 or 7.0 for Windows XP (Carnevale & Hines, 2006) with methods adopted in part from (Schmidt-Hieber *et al.* 2007). Digitized morphological data were imported in NEURON from Neurolucida format (see morphology and immunocytochemistry). Spines were modelled explicitly and consisted of a neck with variable length but fixed diameter of 0.18 μm (Hama *et al.* 1989) and a head with measured size. We did not correct for hidden spines and tissue shrinkage. Segment length was adjusted according to the 'd_lambda rule' by calculation of the alternating current length constant λ at 1 kHz for each section (Carnevale & Hines, 2006; Schmidt-Hieber *et al.* 2007). The integration time step was 50 μs. The specific membrane resistance (R_m), membrane capacitance (C_m) and intracellular resistivity (R_a) were obtained by direct least-squares fitting of the response of the model to the experimental data in NEURON using the built-in 'Brent's principal axis' algorithm that minimizes the sum of squared errors (χ^2). To constrain model parameters, voltage responses to 300 ms current pulses were used and χ^2 was calculated in this period.

Data analysis

Electrophysiological records were analysed using IgorPro (WaveMetrcis, Portland, OR, USA) and FitMaster (Heka). The input resistance (R_{in}) was calculated from the slope of the steady-state current–voltage (I–V) relation from voltage responses of less than ±10 mV from V_{rest}. The membrane time constant (τ_m) was derived by the average of four to six single exponentials fitted to voltage responses to 450 ms current steps. The resting conductance (g_{rest}) was determined in voltage-clamp experiments at holding

potentials of -80 mV and calculated as 1/slope of fitted current–voltage relationships (4 steps of 3 mV). For the calculation of IC_{50} values, fractional block of g_{rest} or of currents at -80 to -140 mV was determined by fitting the values to the Hill curve $y = B + (1 - B)/(1 + (IC_{50}/C)^{\wedge S})$, where y is the g_{rest} or current during or before Ba^{2+}, B is the Ba^{2+}-resistant component and S is the slope. Statistical significance of group differences was measured using Prism 4.0 software (GraphPad, San Diego, CA, USA) applying the following tests: ANOVA plus *post hoc* Tuckey's test for more than two groups with normal distribution, Kruskal–Wallis test plus Dunn's test for more than two groups not normally distributed, Mann–Whitney's test for two groups not normally distributed, Student's *t* tests for two groups normally distributed and Wilcoxon signed rank test for paired tests. Significance of correlation was determined according to a table of Pearson's *r* values. Levels of significance are indicated in figures as * (< 0.05), ** (< 0.01) and *** (< 0.001). Mean values are $\pm$ S.E.M. and numbers represent cells if not mentioned otherwise. Figures were produced using Prism, Illustrator and Photoshop (Adobe, München, Germany).

Results

The intrahippocampal kainate injection mouse model of TLE

Mice with unilateral intrahippocampal KA injections suffered an initial status epilepticus and developed TLE-like AHS with marked GCD in the injected hippocampus, while the contralateral side resembled that of naive mice (Fig. 1*A* and *B*). Morphological analysis revealed a severe loss of neurons especially in the CA1 and CA3c region of the KA-injected hippocampus while the CA3a and CA3b regions still contained viable neurons (Fig. 1*A*, arrow, and *B*). The dentate gyrus showed GCD and was 3- to 4-fold broader as compared to the contralateral side (Fig. 1*A* and *B*). Described data are in good agreement with previous descriptions of the intra-hippocampal KA mouse model of TLE (for details see Suzuki *et al.* 1995; Bouilleret *et al.* 1999; Riban *et al.* 2002; Kralic *et al.* 2005; Le Duigou *et al.* 2005, 2008; Heinrich *et al.* 2006). These previous studies also showed that the anatomical changes develop over the first 2 weeks after KA injection. Therefore, the following results were obtained from animals more than 14 days after injection (except when stated otherwise).

At the cellular level, granule cells on the KA-injected side displayed untypical large proximal excrescences, altered spine morphology, hypertrophic cell bodies and often mossy fibre backsprouting (Figs 1*C*, and 3*A* and *B*) confirming previous observations from KA-injected mice (Suzuki *et al.* 1997) (see below for morphological quantifications). We found at least one basal dendrite per cell in 47 of 62 (75.8%) epileptic cells while none was found in examined control granule cells ($n = 43$).

The input resistance is reduced in epileptic granule cells of kainate-injected mice

Passive membrane properties such as R_{in} and τ_m are important factors for postsynaptic signal integration. The R_{in} is also commonly recorded as a starting routine to test the viability of recorded cells which implies that changes in the passive properties may have been missed in many studies in the selection process. We compared the R_{in} and τ_m values of granule cells from naive mice (control) and KA-injected mice (contralateral and ipsilateral/'epileptic'). To ensure that recorded cells were granule cells they were labelled with biocytin during recordings for *post hoc* anatomical reconstructions and immunocytochemical identification. All recovered cells were positioned in the upper blade of the granule cell layer and had spiny apical dendrites extending into the molecular layer (Fig. 1*C*, Fig. 3*A* and *B*). As the position and morphology of granule cells is altered in KA-injected mice, cells were co-labelled with Prox1, a granule cell marker (Fig. 1*C*) (Liu *et al.* 2000). Prox1-negative cells (4 of 196 recovered cells) were excluded from further analysis. Electrophysiological and morphological properties of control granule cells (Fig. 1*C–F*) matched those previously described for mature granule cells recorded in adult rodents using similar techniques (Staley & Mody, 1992; Schmidt-Hieber *et al.* 2004).

The R_{in} was strongly reduced in epileptic granule cells (Fig. 1*D* and *E*) (control, 421 ± 12 MΩ, $n = 125$; epileptic, 218 ± 5 MΩ, $n = 197$, $P < 0.001$). The R_{in} of granule cells from saline-injected hippocampi was not different from control granule cells ($n = 9$, $P > 0.05$, data not shown). Although V_{rest} values of granule cells were largely overlapping, the mean of 197 epileptic granule cells was 3.4 mV depolarized compared to control cells (control, -81.1 ± 0.5 mV, $n = 125$; epileptic, -77.7 ± 0.4 mV; $n = 197$, $P < 0.001$, see below for discussion on V_{rest}). Since overall contralateral granule cells displayed a morphological and electro-physiological phenotype similar to control granule cells (Fig. 1*C–E*) (V_{rest}: -82.5 ± 1.3 mV, R_{in}: 513 ± 33 MΩ, $n = 21$, $P > 0.05$ *vs.* control, respectively) we compared only control *vs.* epileptic granule cells for the following analyses.

To rule out that differences in recording R_{seal} resulted in erroneous underestimation of epileptic R_{in} values, we verified that the ratio of R_{in}/R_{seal} was sufficiently low to avoid a significant influence on the measured R_{in} (see Methods). To provide extra security against this error, we additionally selected only those cells with a R_{in}/R_{seal} ratio of < 0.1 and these ratios were not different between control

and epileptic granule cells (control, 0.076 ± 0.004, $n = 33$; epileptic, 0.066 ± 0.002, $n = 103$, $P > 0.05$). Even with these stringent criteria the R_{in} difference remained robust (control, 371 ± 22 MΩ, $n = 33$; epileptic, 187 ± 6 MΩ, $n = 103$, $P < 0.001$), suggesting that control and epileptic granule cells did indeed possess a different R_{in}.

The R_{in} change may reflect a decrease in R_m and/or an increase in membrane surface. The τ_m is the product of R_m and C_m. The latter is relatively constant in biological membranes with values around $1\ \mu$F cm^{-2} including those of granule cells (Schmidt-Hieber *et al.* 2007). If this value is assumed to be identical in epileptic granule cells, τ_m is
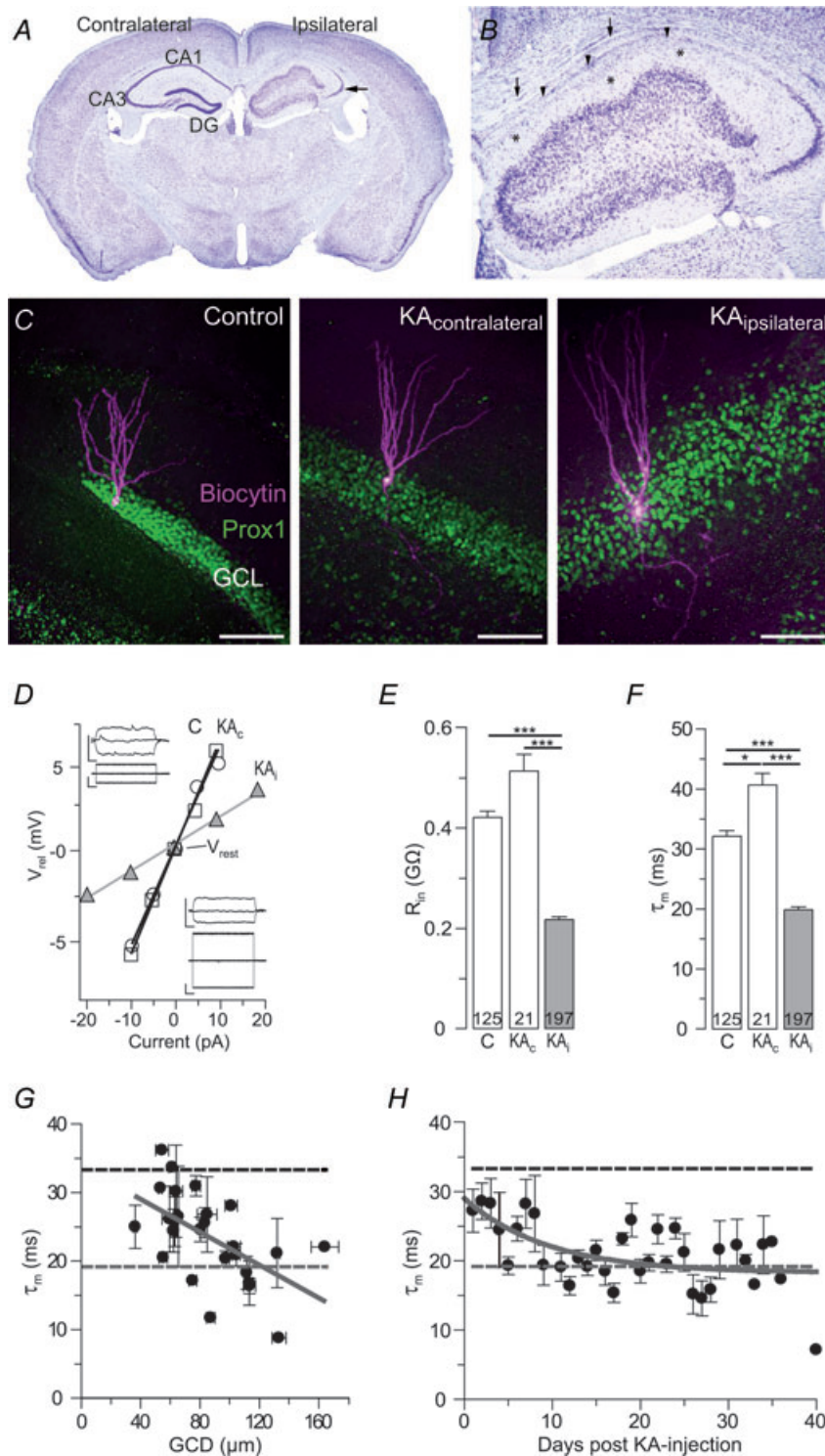

Figure 1. The input resistance is reduced in epileptic granule cells of kainate-injected mice
The input resistance (R_{in}) is reduced in 'epileptic' granule cells of kainate (KA)-injected mice. *A* and *B*, cresyl violet staining of KA-injected (ipsilateral) hippocampi show a complete loss of neurons in the CA1 region (*B*, arrowheads) and a severe loss in the CA3c region of the injected hippocampus. The CA3a and CA3b regions still contained viable neurons (*A* arrow, *B*). The dentate gyrus granule cell layer (DG) of the injected hippocampus is 3- to 4-fold broader, displaying largely dispersed cells in this area (GCD). Note that the molecular layer of the DG can still be separated from the former outer stratum lacunosum-moleculare via residual capillaries (*B*, asterisks; see also Fig. 7*A1* and *C2*). The upper border of the CA1 region against the corpus callosum is also visible (*B*, arrows). *C*, biocytin-labelled granule cells of control and KA-injected mice (KA, contralateral and ipsilateral, respectively) co-labelled with the granule cell marker Prox-1. Scale bars, 100 μm. *D*, current–voltage relation of control (*C*, open circles), contralateral and epileptic granule cells of the KA-injected mice (KA$_c$, open squares, and KA$_i$, grey triangles, respectively) as it was used for the calculation of R_{in} in *E*. V_{rel}, voltage relative to the resting membrane potential (V_{rest}). Insets, current-clamp recordings of granule cells shown in *C*. Upper and lower traces, voltage and current traces, respectively. Scale bars, 0.2 s, 10 mV, 10 pA. *E* and *F*, R_{in} values and membrane time constants (*F*, τ_m) were both decreased in KA$_i$ granule cells compared to KA$_c$ and control granule cells. *G* and *H*, τ_m values of KA$_i$ granule cells decreased in correlation with the degree of GCD (*G*, width of granule cell layer averaged per respective slice) in particular during the first 2 weeks after KA injection (*H*). Several days post KA, τ_m values were control-like, but decreased subsequently and stabilized at low levels 30–40 days post-KA. All values are mean $\pm$ s.e.m. Values in bars are number of cells.

independent of membrane surface and can consequently be used as a direct estimate of R_m. In epileptic granule cells, τ_m values were strongly reduced compared to control cells (Fig. 1F) (control, 32.2 ± 0.9 ms, $n = 125$; epileptic, 19.9 ± 0.5 ms, $n = 197$, $P < 0.001$). Contralateral cells possessed slightly larger τ_m values than control granule cells (Fig. 1F), an interesting difference we have not further investigated here. Importantly, the low τ_m values of epileptic granule cells indicate that the reduced R_{in} was not due to an increased membrane surface (see also morphological analysis below). Instead, the data suggest a reduction of R_m by approximately 10 kΩ cm^2 at V_{rest}.

In humans and KA-injected mice, GCD can be used as a measure of TLE-related hippocampal damage (Houser, 1990; Suzuki et al. 1995; Bouilleret et al. 1999; Thom et al. 2002; Heinrich et al. 2006). To test whether the changes in passive properties correlate with the extent of GCD we recorded granule cells 1–14 days after KA injection, as in this period AHS and GCD progressively develop (Suzuki et al. 1995; Bouilleret et al. 1999; Heinrich et al. 2006). Indeed, R_{in} and τ_m values negatively correlated with the degree of GCD (Fig. 1G) (τ_m vs. GCD, $r = 0.56$, $n = 26$ slices, $P < 0.01$), comparable to our results from TLE patients (Stegen et al. 2009). Following the first 2 weeks post-KA injection, during which τ_m gradually decreased (Fig. 1H) ($r = 0.75$, $n = 13$ days, $P < 0.01$), the R_{in} and τ_m values remained relatively constant for the rest of the testing period (Fig. 1H) (post-KA days 15–40, $r = 0.36$, $n = 22$, $P = 0.10$). In control mice, R_{in} did not correlate with the age of the animal ($r = 0.15$, $n = 125$, $P = 0.10$, data not shown).

In summary, these data show that the R_m of granule cells in the sclerotic focus becomes substantially reduced with increasing AHS and GCD. In other words, our results suggest that the membrane leak conductivity increases in parallel to epileptogenesis during which morphological, electroencephalographic and behavioural symptoms of the chronic epileptic condition have been shown to gradually develop (Suzuki et al. 1995; Bouilleret et al. 1999; Riban et al. 2002; Kralic et al. 2005; Le Duigou et al. 2005, 2008; Heinrich et al. 2006).

The excitability is reduced in 'epileptic' granule cells of kainate-injected mice

Ohm's law ($R = U/I$) predicts that the reduced R_{in} of epileptic granule cells should lead to a decreased excitability, i.e. more current should be necessary to evoke action potential firing. We tested this hypothesis by measuring the minimal current injection needed to trigger at least one action potential (rheobase) (Fig. 2). The rheobase was approximately 3-fold increased in epileptic compared to control granule cells, confirming the predicted decrease in excitability (Fig. 2A–C) (rheobase:

control, 70 ± 6 pA, $n = 32$; epileptic, 228 ± 9 pA, $n = 87$, $P < 0.001$). Epileptic granule cells also showed a ramp-shaped delay before the first action potential (Fig. 2B). The mechanism underlying this difference was not further analysed here, but important for the present study is that current injections triggering strong activity in control cells were well below the potential needed to even start the ramp-shaped delay in epileptic cells. In fact, control granule cells were occasionally killed with current amplitudes used to evoke spiking in epileptic granule cells. Consistent with the hypothesis that the low R_{in} critically diminished the propensity of epileptic granule cells to generate action potentials, there was a clear relation between the R_{in} and the rheobase (Fig. 2D)
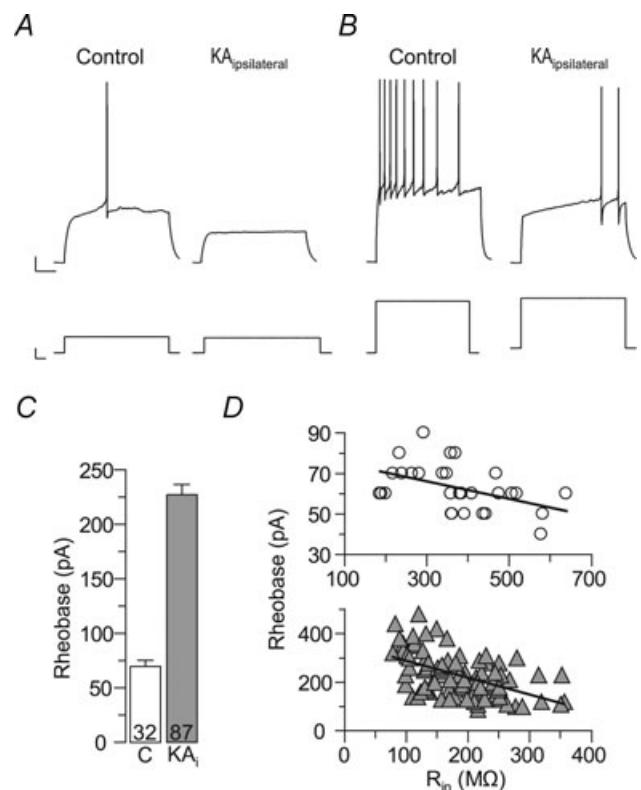

Figure 2. The excitability is reduced in epileptic granule cells of kainate-injected mice
Epileptic granule cells of KA-injected (ipsilateral) hippocampi need more depolarizing current to generate action potentials (APs). A, a small current injection was sufficient to evoke an AP in control granule cells (left panel), but not in epileptic granule cells (right panel). B, the current needed to evoke minimal AP firing in epileptic granule cells (right panel) either killed control granule cells (not shown) or evoked strong AP firing in control cells (left panel). C, summary of experiments as in A and B. The current needed to generate at least one AP (rheobase) was strongly increased in epileptic granule cells (KA$_i$). D, the rheobase was related to the R_{in}, suggesting that the latter was responsible for the reduced excitability of epileptic granule cells. Upper panel (circles), control granule cells; lower panel (grey triangles), epileptic granule cells). Note different y and x axis scales in these panels.
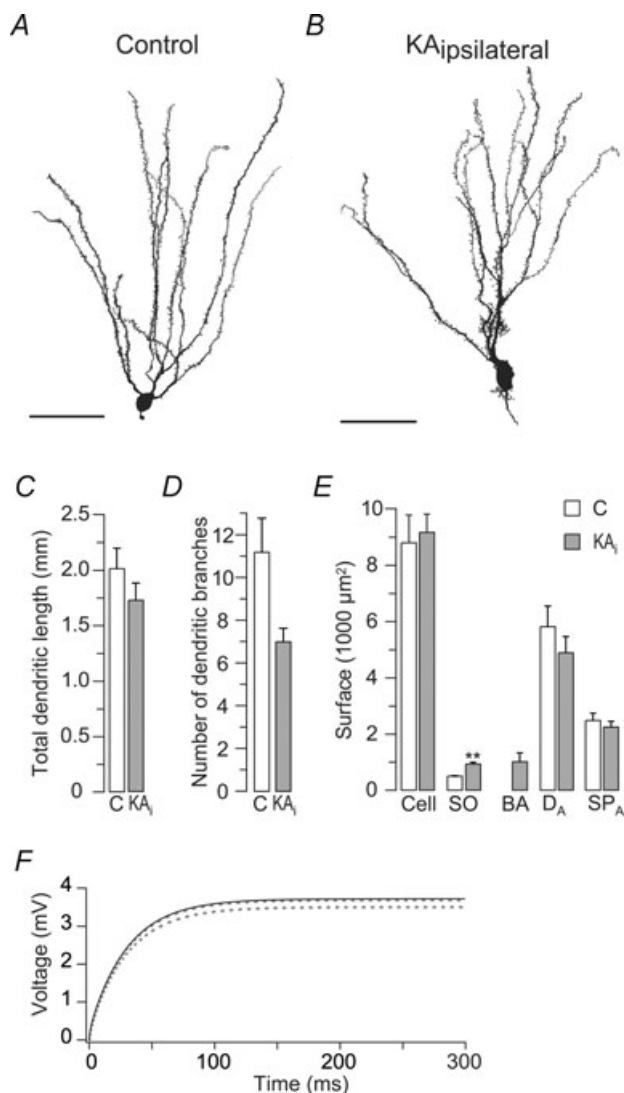
A Control

B KA$_{ipsilateral}$

(control, $r = 0.46$, $n = 32$, $P < 0.05$; epileptic, $r = 0.52$, $n = 87$, $P < 0.001$). These results suggest that the excitability of epileptic granule cells from the sclerotic hippocampus is decreased rather than increased.

Changes in membrane morphology are not responsible for the decreased input resistance of epileptic granule cells

Although the reduced τ_m values of epileptic granule cells indicated that the reduced R_{in} was not due to an increased membrane surface, this interpretation depends on the assumption of a constant C_m (see above). To independently verify the interpretation we directly quantified the membrane surface of recorded and identified granule cells using 3-D reconstruction from confocal image stacks of biocytin-labelled cells via the software Neurolucida (Fig. 3*A* and *B*). The accumulated length of all dendritic branches, the 'total dendritic length' (TDL), was not significantly different in epileptic and control cells (Fig. 3*C*) (control, $2012 \pm 186 \, \mu$m, $n = 5$; epileptic, $1724 \pm 156 \, \mu$m, $n = 5$, $P = 0.31$). Epileptic granule cells had a slightly reduced number of dendritic branches especially in the first three branch orders (Fig. 3*D*) (control, 11.2 ± 1.6, $n = 5$; epileptic, 7.0 ± 0.6, $n = 5$, $P = 0.056$), but an increase in surface from basal dendrites, dendritic excrescences and enlarged somata (Fig. 3*E*, 'SO') (control, $492 \pm 20 \, \mu$m^2, $n = 5$; epileptic, $926 \pm 58 \, \mu$m^2, $n = 5$, $P < 0.01$). The previously noted proximal surface increase (Suzuki *et al.* 1997) apparently was compensated by the reduced number of apical branches such that the total membrane surface of reconstructed granule cells was not significantly different (Fig. 3*E*, 'Cell') (control, $8799 \pm 978 \, \mu$m^2; epileptic, $9173 \pm 649 \, \mu$m^2, $P = 0.55$). Also, the total surface of spines was similar (Fig. 3*E*, 'SP$_A$') (control, $2477 \pm 257 \, \mu$m^2, $n = 5$; epileptic, $2249 \pm 207 \, \mu$m^2, $n = 5$, $P = 0.69$). However, their distribution was changed: proximally, the density of spines was increased in epileptic granule cells in particular when basal dendrites where included (1st branch order: control, $0.055 \pm 0.04 \, 1 \, \mu$m^{-1}, $n = 5$; epileptic, $0.398 \pm 0.03 \, 1 \, \mu$m^{-1}, $n = 5$; $P < 0.01$), while on distal dendrites the opposite effect was observable (4th branch order: control, $0.770 \pm 0.043 \, 1 \, \mu$m^{-1}, $n = 5$; epileptic, $0.566 \pm 0.054 \, 1 \, \mu$m^{-1}, $n = 5$; $P < 0.05$). Hidden spines were not considered in this analysis. Importantly, the recorded R_{in} of the same reconstructed granule cells with similar total membrane surfaces was significantly lower in epileptic *vs.* control neurons (control, 402 ± 57 MΩ; epileptic, 249 ± 29 MΩ, $n = 5$, $P < 0.05$), suggesting that the decrease in R_{in} was not due to an increase in membrane surface.

Although granule cells are generally considered electrotonically very compact (such that the determination

Figure 3. Changes in membrane morphology are not responsible for the decreased input resistance of epileptic granule cells

Quantitative morphology and cable modelling of control and epileptic granule cells. *A* and *B*, Neurolucida reconstructions of a control (*A*) and an epileptic (*B*) granule cell showing morphological changes as previously described (see text). Scale bars, 50 μm. *C*, the total dendritic length was not significantly different in control and epileptic (KA$_i$) granule cells ($n = 5$, respectively). *D*, the number of dendritic branches (1–3 branch order) was slightly reduced in epileptic granule cells. *E*, membrane surface quantification of sub-compartments showing that the total membrane surface (Cell) and the surface of apical dendrites (D$_A$) and spines (SP$_A$) was similar, while somata (SO) were enlarged in epileptic granule cells. Basal dendrites (BA) include spines. *F*, computer simulation of the passive cable properties of reconstructed granule cells to test the influence of changes in geometry on the R_{in}. Passive cable parameters R_m, R_a and C_m of the control granule cell shown in *A* were fitted to its charging curve evoked by 10 pA (black line). Fitted control parameters were then implemented in the cable model from reconstructed epileptic granule cell shown in *B*. The resulting 'hybrid' cell with epileptic geometry but control cable properties showed no obvious changes in the charging curve (lower dashed line). Correcting for the slight difference in total membrane surfaces resulted in identical charging curves (upper dashed line), suggesting that the measured R_{in} reduction was not due to the changed geometry.

of R_{in} at steady state should be possible without a contribution of so-called space-clamp artefacts and sub-cellular morphology changes), it is theoretically possible that the disproportional change of proximal vs. distal surface affected the R_{in} of granule cells independently of changes in total membrane surface. To supply an estimate of such a potential impact of cell geometry on R_{in} we computed passive cable models using the morphology of reconstructed granule cells obtained from the above 3-D reconstructions (see Methods). If changes in geometry independent of total surface were responsible for the reduced R_{in} of epileptic granule cells, then transferring the passive cable properties (R_m, R_a and C_m) from a control cell to the morphology of an epileptic cell with similar total surface should reduce the R_{in} considerably. Using NEURON we fitted the parameters R_m, R_a and C_m to the voltage responses of the control cell shown in Fig. 3A (R_{in}, 375 MΩ, τ_m, 31 ms, surface, 8771 μm^2). The resulting fit is shown in Fig. 3F (black upper line). The passive parameters obtained from the fit (R_m, 30.4 kΩcm^2, R_a, 287 Ωcm, C_m, 1.00 μF cm^{-2}) were in good agreement with previous cable models of granule cells (Schmidt-Hieber et al. 2007). For epileptic granule cells no such reference exists, therefore we refrained from fitting their parameters. The control parameters were then implemented in the model of the reconstructed epileptic cell shown in Fig. 3B which in the patch-clamp recording had the typical low R_{in} of epileptic granule cells (R_{in}, 228 MΩ, τ_m, 22 ms, surface, 9237 μm^2). The resulting 'hybrid' model cell with control-like cable properties but epileptic morphology possessed a charging curve similar to the control cell (Fig. 3F, lower dashed line) and accordingly very similar R_{in} and τ_m values (model cells: control, R_{in}, 378 MΩ, epileptic, R_{in}, 355 MΩ, control, τ_m, 30 ms, epileptic, τ_m, 30 ms). As the epileptic cell had a slightly larger membrane surface (factor 1.053), we scaled the charging curve by this factor to correct for the small surface effect. The resulting charging curve was now virtually identical to that of the control cell model (Fig. 3F, upper dashed line).

In summary, the combined results of this section strongly support our conclusion (from τ_m measurements) that neither the changes in membrane surface nor changes in the geometry were responsible for the reduced R_{in} of epileptic granule cells. By contrast, the main factor was an increase in membrane conductivity.

A potassium conductance is increased in epileptic granule cells

To obtain more information about the conductance underlying the decreased R_{in} of epileptic granule cells we characterized the pharmacology of the resting conductance measured by fitting the slope of the I–V relation recorded in voltage clamp at a holding potential of −80 mV ('g_{rest}') (Fig. 4A). These experiments were conducted in ACSF containing antagonists of Na$^+$ channels (TTX, 0.5 μM), AMPA receptors (CNQX, 20 μM) and NMDA receptors (AP-5, 50 μM). These drugs did not affect the g_{rest} significantly (sensitive g_{rest}: control, −0.083 ± 0.088 nS, $n = 8$; epileptic, −0.078 ± 0.165 nS, $n = 17$, $P = 0.98$) suggesting that glutamatergic events, for example, by tonic NMDA receptor activation (Isokawa & Mello, 1991), did not contribute to the g_{rest}. Overall, the g_{rest} of epileptic granule cells was increased by a factor of ∼2.2 (by 2.79 nS) compared to control cells (see Fig. 5C, left panel) (control, 2.41 ± 0.16 nS, $n = 28$; epileptic 5.20 ± 0.34 nS, $n = 25$, $P < 0.001$).

When the intracellular and extracellular K$^+$ was replaced with TEA$^+$ (via re-patching, see Methods), the g_{rest} of control granule cells was reduced by 1.32 ± 0.22 nS (Fig. 4B and C) (control, from 2.34 ± 0.30 nS to 1.03 ± 0.14 nS, $n = 4$, $P < 0.05$). In epileptic granule cells, K$^+$ replacement decreased the g_{rest} by 3.70 ± 0.65 nS (Fig. 4B and C) (epileptic, from 5.28 ± 0.75 nS to 1.58 ± 0.24 nS, $n = 6$, $P < 0.01$). Accordingly, the K$^+$-sensitive g_{rest} was 2.8 times higher in epileptic compared to control granule cells (difference, 2.38 nS, $P < 0.01$). The g_{rest} values of epileptic granule cells were still enlarged after K$^+$ replacement although the difference was not significant anymore (Fig. 4B) (control, 1.03 ± 0.14 nS, $n = 4$; epileptic, 1.63 ± 0.26 nS, $n = 5$, $P = 0.19$). Numbers of epileptic cells are unequal, because in one case picrotoxin was present throughout the experiment which could affect the K$^+$-insensitive g_{rest} (but not the K$^+$-sensitive g_{rest}). When using the initial difference in g_{rest} averaged for these experiments (2.94 nS) as 100%, the difference in K$^+$-sensitive g_{rest} (2.38 nS) amounted to 80.9%. This suggests that K$^+$ conductances accounted for most of the R_{in} difference (see below for further assessment of the relative contributions to the increased g_{rest}). Indeed, the amount of K$^+$-sensitive g_{rest} correlated with the R_{in} of these cells and had a hyperbolic relation (Fig. 4D) ($r = 0.97$, $n = 10$, $P < 0.01$). By subtraction of the currents following K$^+$ replacement from those before K$^+$ replacement, the I–V relationship of 'K$^+$ currents' was obtained (Fig. 4E). Consistent with flux through K$^+$ channels, these currents reversed close to the Nernst equilibrium potential of K$^+$ ions (E_K: −104 mV; control, −104.3 mV; epileptic −100.0 mV). Figure 4E also shows that there was a disproportionate increase in inward K$^+$ currents compared to outward K$^+$ currents in epileptic granule cells.

Barium- and bicuculline-sensitive components underlie the increased resting conductance of epileptic granule cells

Many mechanisms may contribute to the resting leak conductance of neurons, but K$^+$ and Cl$^-$ channels are

the most likely ones. The shape of the K^+ current $I–V$ (Fig. 4E) suggested Ba^{2+}-sensitive inward rectifier K^+ (Kir) channels as good candidates (Goldstein *et al.* 2001; Stanfield *et al.* 2002). In addition, tonic $GABA_A$ activation may be increased in granule cells during TLE (Nusser *et al.* 1998; Bouilleret *et al.* 2000; Loup *et al.* 2000; Farrant & Nusser, 2005). Therefore we tested the effect of Ba^{2+} (200 μM) and $GABA_A$ inhibitors bicuculline (BMI, 20 μM) or picrotoxin (PTX, 100 μM) on the g_{rest} of epileptic and control granule cells (Fig. 5). These experiments were conducted in ACSF containing TTX, CNQX and AP-5.

Application of BMI or PTX did not significantly reduce the g_{rest} in control granule cells (Fig. 5$A–C$) (BMI, from 2.94 ± 0.29 nS to 2.70 ± 0.30 nS; BMI-sensitive g_{rest}, 0.23 ± 0.21 nS, $n = 4$, $P = 0.125$; PTX-sensitive g_{rest}, 0.31 ± 0.12 nS, $n = 5$, $P = 0.22$) and the holding current necessary to keep the cells hyperpolarized at -90 mV was not changed (from -26 ± 9 pA to -29 ± 12 pA, $n = 4$, $P = 0.63$, not shown). This is consistent with previous results suggesting that in hippocampal slices of adult animals tonic $GABA_A$ current has little effect on the R_{in} and is small unless artificially increased by pharmacological manipulations such as elevating the extracellular GABA concentration (Stell *et al.* 2003; Farrant & Nusser, 2005; Glykys *et al.* 2008).

However, in epileptic granule cells the g_{rest} was clearly reduced by bicuculline or picrotoxin (Fig. 5$A–C$) (BMI, from 5.23 ± 0.45 nS to 4.30 ± 0.41 nS; BMI-sensitive g_{rest}, 0.93 ± 0.06 nS, $n = 6$, $P < 0.05$; PTX-sensitive g_{rest}, 1.18 ± 0.22 nS, $n = 7$, $P < 0.05$) and the holding current necessary to keep the cells hyperpolarized at -90 mV was slightly though not significantly decreased (from -30 ± 14 pA to -19 ± 15 pA, $n = 5$, $P = 0.063$, not shown). These results suggest that in contrast to control granule cells, in epileptic granule cells, a $GABA_A$ conductance contributed to the g_{rest} (difference: BMI, 0.70 nS, $P < 0.01$; PTX, 0.87 nS, $P < 0.01$). Note that this difference corresponds roughly to the g_{rest} difference remaining after K^+ removal (0.6 nS, see above). When using the initial difference in g_{rest} averaged for these experiments (2.29 nS) as 100%, the difference in BMI-sensitive g_{rest} (0.70 nS) amounted to 30.6%. The apparent discrepancy to the $\sim$20% non-K^+ g_{rest} mentioned above is probably due to the variability across experiments (see also below). The employed ion concentrations determine that Cl^- currents should have a depolarizing influence and also under undisturbed intra-cellular conditions $GABA_A$ is depolarizing in granule cells (Staley & Mody, 1992; Soltesz & Mody, 1994). Consistent with this, the application of PTX hyperpolarized epileptic
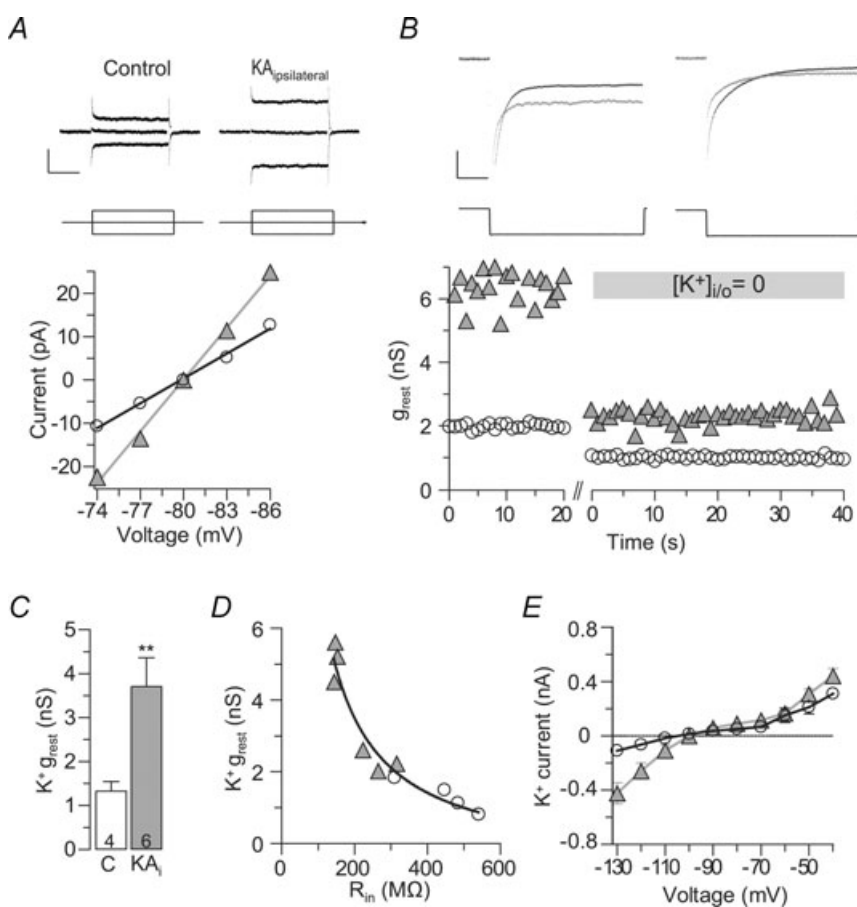

Figure 4. A potassium conductance is increased in epileptic granule cells

K^+ replacement experiments showing the contribution of K^+ ions to the resting leak conductance (g_{rest}) of granule cells. *A*, the g_{rest} was determined in voltage-clamp recordings as the fitted slope of $I–V$ relations at -80 mV holding potential (control and epileptic, white circles and grey triangles, respectively). Sample current traces of control and epileptic granule cells (upper black traces) in response to ± 6 mV voltage commands shown below. These experiments were conducted in the presence of TTX, CNQX and AP-5. Scale bars, 0.2 s, 20 pA. *B*, overlaid current responses of control and epileptic granule cell during the replacement of the entire intracellular and extracellular K^+ ($[K^+]_{i/o} = 0$). *x*-axis break indicates re-patching of cell with new intracellular solution. Sample current responses to -5 mV voltage pulses for each condition are shown in the upper panels (black, control; grey, epileptic). Scale bars, 20 pA, 20 ms. *C*, summary of experiments as in *B* (C, control, KA_i, epileptic). *D*, the amount of K^+-dependent g_{rest} correlated with the initial input resistance (R_{in}) of granule cells in hyperbolic manner. *E*, K^+ current family obtained by subtraction of currents after K^+ replacement from those before the replacement. Currents were evoked by voltage commands decreasing with 10 mV steps. Values in bars are numbers of cells.

granule cells (from -76.9 ± 1.7 to -82.0 ± 2.1 mV, $n = 8$, $P < 0.05$) and PTX- or BMI-sensitive currents had a depolarizing reversal potential in epileptic granule cells (E_{PTX}, -62 mV; E_{BMI}, -67 mV, not shown).

Subsequent to BMI we applied 200 μM Ba^{2+} which inhibited a major component of g_{rest}. Notably, the effect was 1.7-fold in epileptic compared to control granule cells (Fig. 5*A–C*) (g_{rest} sensitive to 200 μM Ba^{2+}: control, 0.96 ± 0.07 nS, $n = 11$; epileptic, 1.66 ± 0.17 nS, $n = 9$, $P < 0.01$). The subsequent application of 5 mM Cs^+ had minor additional effects (Fig. 5*A–C*) (Cs^+ in the presence of BMI and 200 μM Ba^{2+}, sensitive g_{rest}: control, 0.16 ± 0.01 nS, $n = 2$; epileptic, 0.35 ± 0.17 nS, $n = 4$).

We further quantified the Ba^{2+} sensitivity of g_{rest} in the presence of TTX, CNQX, AP-5 and PTX. At 40 μM, the Ba^{2+}-sensitive g_{rest} was still more than 2-fold in epileptic granule cells (Fig. 5*C*) (control 0.35 ± 0.07 nS, $n = 6$; epileptic 0.98 ± 0.22 nS, $n = 6$, $P < 0.01$). The IC_{50} of the sensitive g_{rest} was in the micromolar range (Fig. 5*D*) (IC_{50} of $g_{rest} \pm$ s.d.: control, 79.8 ± 15.2 μM, $n = 39$; epileptic, 122.3 ± 43.2 μM, $n = 34$), but at these potentials approximately half of g_{rest} was not sensitive to 1 mM Ba^{2+} (Fig. 5*C*) (sensitive g_{rest} 1 mM: control 1.10 ± 0.19 nS, $n = 7$; epileptic 2.41 ± 0.44 nS, $n = 5$, $P < 0.05$). Importantly, similar to our K^+ replacement experiments, it was the Ba^{2+}-sensitive g_{rest} that correlated with the initial R_{in} and had a hyperbolic relation (Fig. 5*E*) (1 mM, $r = 0.97$, $n = 17$, $P < 0.01$) consistent with the hypothesis that the Ba^{2+}-sensitive conductance controlled the R_{in}.

In summary, several leak conductances appear upregulated in epileptic granule cells. Most prominent is the increase in a K^+ resting conductance. In addition, a $GABA_A$ leak appears in epileptic granule cells. It is difficult to give an estimate of the relative contributions to the increased leak, because comparisons are only possible across cells and animals (and the variability between cells is high). Stressing this concern, we nevertheless offer a rough estimate, the result of which depends on the g_{rest} difference between epileptic and control granule cells used as 100%. According to the K^+ removal experiments, the relative contribution of K^+ conductances (2.38 nS) is 80%, leaving 20% non-K^+ conductance. According to the BMI experiments, a $GABA_A$ conductance (0.70 nS) accounted for 30% leaving 70% for the K^+ conductance. Thus, in combination, a reasonable estimate for the pathological leak conductance appears to be: K^+, 70–80% and $GABA_A$, 20–30%.

The upregulated K^+ leak consists of a component with high and a component with low Ba^{2+} sensitivity. Approximately 55.0% were sensitive to 1 mM Ba^{2+} at V_{rest} (1.31 nS, ~47.0% of total). Thus, there was an additional K^+ leak which was not sensitive to Ba^{2+} concentrations below 1 mM (~45%) at V_{rest}.

Additional pharmacology of the resting conductance of epileptic granule cells

To assess whether other ion channels contribute to the increased g_{rest} of epileptic granule cells, in particular the component with low Ba^{2+} sensitivity, we tested various channel inhibitors. However, none of these tests resulted in evidence for an additional leak mechanism. The following inhibitors of K^+ channels (Coetzee *et al.* 1999; Patel & Honore, 2001; Kubo *et al.* 2005) did not significantly reduce the g_{rest} of epileptic granule cells or the effect was not significantly different between epileptic and control cells (listed is the drug-sensitive g_{rest}): tertiapin, an inhibitor of Kir1.1, Kir3.1, Kir3.2 and Kir3.4 channels ($0.05–1$ μM, -0.01 ± 0.07 nS, $n = 5$); bupivacaine, an inhibitor of Kir3 and some K2P channels (1 mM, control, 0.92 ± 0.36 nS, $n = 3$; epileptic, 0.65 ± 0.16 nS, $n = 5$); 4-AP, an inhibitor of fast inactivating voltage-gated K^+ (Kv) channels (4 mM, 0.24 ± 0.10 nS, $n = 4$); TEA, an inhibitor of slowly inactivating Kv channels and big conductance Ca^{2+}-sensitive K^+ channels ($10–20$ mM, 0.26 ± 0.32 nS, $n = 5$); XE991 and linopirdine, inhibitors of M-current-mediating Kv7 (KCNQ) K^+ channels ($10–250$ μM, 0.40 ± 0.35 nS, $n = 4$; 100 μM, 0.20 ± 0.14 nS, $n = 4$, respectively); apamin, an inhibitor of small conductance Ca^{2+}-activated K^+ channels (500 nM, 0.15 ± 0.18 nS, $n = 2$) and tolbutamide, an inhibitor of ATP-sensitive Kir (Kir6) channels (500 μM, -0.17 ± 0.33 nS, $n = 3$). Lowering the pH to 6.5, which should affect acid-sensitive K2P (Task) channels (Patel & Honore, 2001), also did not differentially affect the g_{rest} of control and epileptic cells (control, 0.68 ± 0.26 nS, $n = 5$; epileptic, 0.53 ± 0.15 nS, $n = 11$). Hyperpolarization-activated, cyclic nucleotide-gated cation (HCN) channels which mediate the 'I_h' current may also contribute to a membrane leak although only small I_h currents have been measured in granule cells (Brauer *et al.* 2001). Application of ZD7288 did affect the g_{rest} of epileptic granule cells; however, this effect was similar in control and epileptic granule cells (50 μM, control, 1.14 ± 0.13 nS, $n = 3$; epileptic, 1.19 ± 0.25 nS, $n = 5$), indicating that I_h does not mediate the increase in g_{rest}. We have no evidence that $GABA_B$ receptor-mediated currents (other than Kir3-mediated, see above) contribute to the increased g_{rest} of epileptic granule cells as the antagonist phaclofen had little effect (500 μM, -0.22 ± 0.38 nS, $n = 2$). Overall, these data suggest that the mentioned mechanisms are unlikely to be main players in the increased g_{rest} of epileptic granule cells. Therefore, we did not further investigate these channels in control cells and with respect to the K^+ conductance increased in epileptic granule cells, Kir channels were still the best candidates.
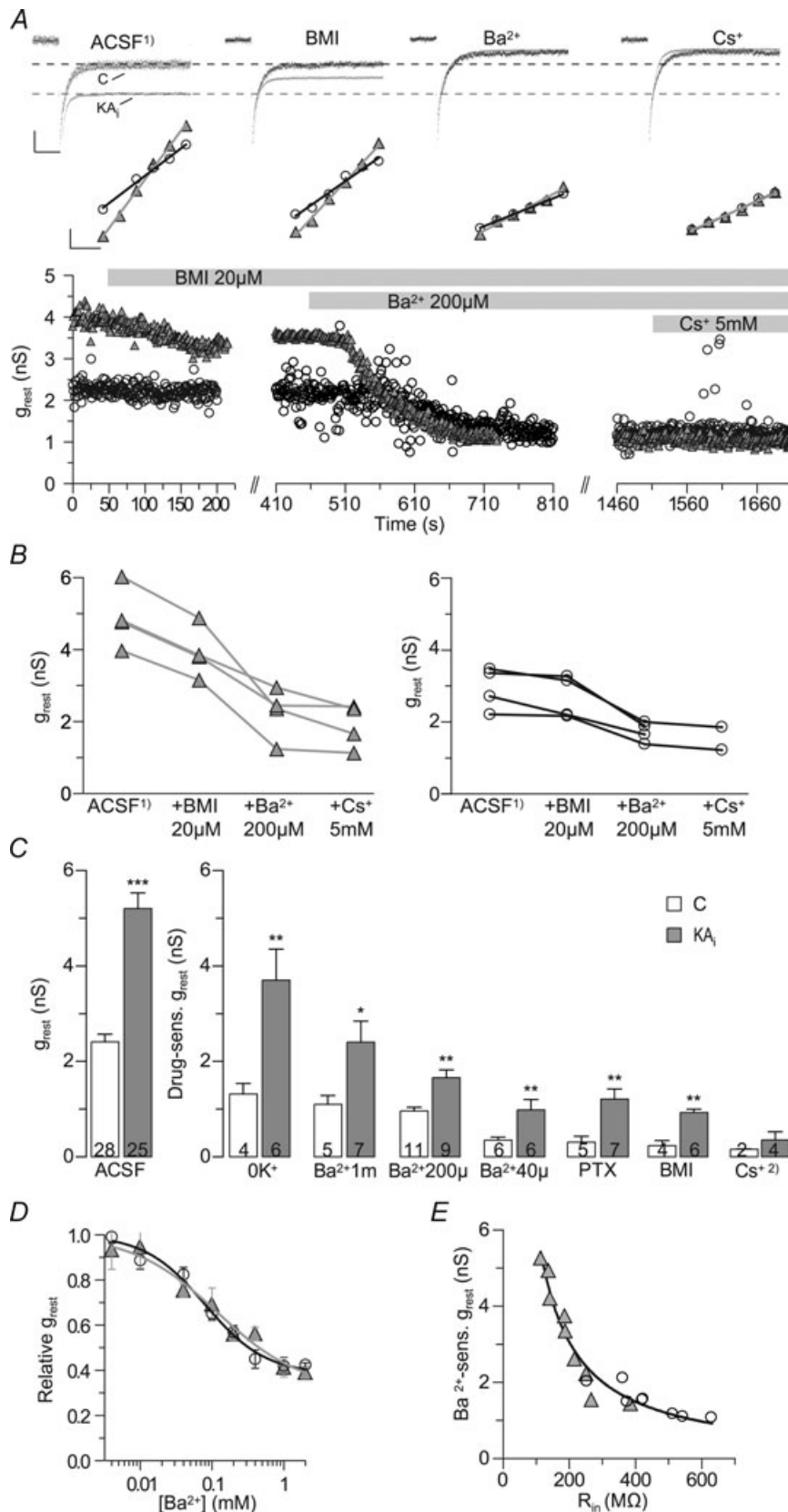
Figure 5. Barium- and bicuculline-sensitive components underlie the increased resting conductance of epileptic granule cells

Successive bicuculline (BMI) and Ba^{2+} application show the relative components responsible for the increased resting conductance (g_{rest}) of epileptic granule cells. *A*, upper panels show superimposed averaged sample currents (evoked by -5 mV pulses) of control (C) and epileptic granule cells for each of the successively applied pharmacological condition shown in the lower panel (black traces and open circles, control; grey traces 'KA$_i$' and triangles, epileptic). Middle panels show fitted *I–V* plots for each condition as used for the calculation of g_{rest} values. The initial application of Na^+ channel and glutamate receptor blockers (ACSF[1]): 0.5 μM TTX, 20 μM CNQX, 50 μM AP-5) did not change the g_{rest} of control and epileptic granule cells (not shown). Additional inhibition of GABA$_A$ receptors (BMI, 20 μM) reduced the g_{rest} in epileptic granule cells but not in control granule cells. Additional application of 200 μM Ba^{2+} inhibited a major component of the g_{rest} in epileptic but also reduced the leak in control granule cells. Additional application of 5 mM Cs^+ had only minimal further effects. Dashed lines in upper panel indicate current levels in the ACSF[1] condition. Scale bars: upper panel, 10 pA, 20 ms; middle panel, 10 pA, 5 mV. *B*, summary of experiments as in *A* showing that 200 μM Ba^{2+} had a larger effect on g_{rest} than BMI. *C*, g_{rest} differences in control and epileptic granule cells (white and grey bars, respectively) and their relative drug sensitivities. $Cs^{+2)}$, as Cs^+ was applied in addition to 200 μM Ba^{2+}, only a minor additional effect appeared. *D*, inhibition of g_{rest} by Ba^{2+} was described by a Hill function. $IC_{50} \pm$ s.d. values, Hill coefficients and relative base levels were 79.8 ± 15.2 μM, -1.03 and 0.38 for control granule cells ($n = 39$) and 122.3 ± 43.2 μM, -0.77 and 0.32 for epileptic granule cells ($n = 34$), respectively, suggesting that $\sim$32% of the epileptic g_{rest} were Ba^{2+} insensitive even to millimolar concentrations. These experiments were conducted in the presence of TTX, CNQX, AP-5 and PTX. *E*, the Ba^{2+}-sensitive g_{rest} correlated with the respective initial R_{in} of control and epileptic granule cells (open circles and grey triangles, respectively) consistent with the hypothesis that this conductance controls the R_{in}. Values in bars are numbers of cells.

Inwardly rectifying currents with properties of Kir2 channels are increased in epileptic granule cells

The above results suggested that in particular in epileptic granule cells, but also in control granule cells, one conductance controlling the R_{in} of granule cells is highly Ba^{2+} sensitive. In particular, 'classic' or 'resting' Kir (Irk1–4/Kir2.1–2.4) channels are known to possess high open probabilities around V_{rest} and have Ba^{2+} sensitivities in the micromolar range (Stanfield *et al.* 2002; Kubo *et al.* 2005). However, around V_{rest}, where the above g_{rest} data were collected, Kir2 conductances are likely to be mixed with other conductances and pharmacological characteristics are usually determined at unphysiologically hyperpolarized potentials. To better isolate and compare the properties of Kir conductances of granule cells we therefore analysed Ba^{2+} sensitivity of Kir currents at hyperpolarized potentials in the presence of TTX, CNQX, AP-5 and PTX.

Subtracting voltage-evoked currents after application of 40 μM Ba^{2+} from those before application resulted in currents with marked inward rectification (Fig. 6*A* and *B*). Importantly, these Kir currents were of clearly increased amplitudes in epileptic granule cells (Fig. 6*A* and *B*) (e.g. at -120 mV, control, 58 ± 19 pA, $n = 6$; epileptic, 134 ± 20 pA, $n = 6$, $P < 0.05$). In addition, a linear component insensitive to 40 μM Ba^{2+} was also increased (Fig. 6*B* inset). In both control and epileptic granule cells, the Ba^{2+}-insensitive currents decreased with hyperpolarization. This is evident when comparing the dose–response curve of g_{rest} (Fig. 5*D*) to the dose–response curve of evoked currents at -120 mV (Fig. 6*C*). At

-120 mV approximately 75% of currents were blocked by Ba^{2+} concentrations below 0.5 mM ($IC_{50} \pm$ S.D., control, $14.3 \pm 1.5 \mu$M, $n = 37$; epileptic, $19.2 \pm 2.3 \mu$M, $n = 34$), which is similar to sensitivities of Kir2 channels (Preisig-Muller *et al.* 2002; Schram *et al.* 2002). It is known that the sensitivity of Kir currents to Ba^{2+} decreases with depolarization (Preisig-Muller *et al.* 2002; Schram *et al.* 2002) and we also measured this effect (Fig. 6*D*). This could mean that the contribution of Kir channels to the leak conductance may be underestimated when judged by the Ba^{2+} sensitivity of g_{rest}.

In summary, inwardly rectifying currents were significantly increased in epileptic granule cells and the biophysical and pharmacological profile indicated Kir2 channels as the most likely candidates for these currents. We tested this hypothesis by immunocytochemical localization of Kir2 channel subunits.

Kir2 channel proteins are elevated in epileptic granule cells

All proteins of the Kir2 (Kir2.1–2.4) channel family are present in moderate to high levels in the granule cell layer (Karschin *et al.* 1996; Liao *et al.* 1996; Pruss *et al.* 2005), but no morphological data on their expression in relation to AHS were available. Using antibodies with well characterized specificity (Pruss *et al.* 2003), we found all four Kir2 subunit proteins at elevated levels in the epileptic compared to the contralateral granule cell layer (Fig. 7*A*–*D*), supporting our electrophysiological data. Although precise quantification of protein levels via an

Figure 6. Inwardly rectifying currents with properties of Kir2 channels are increased in epileptic granule cells
Inward currents were highly Ba^{2+} sensitive and strongly increased in epileptic granule cells. *A*, subtraction traces of currents sensitive to 40 μM Ba^{2+} in a control and epileptic granule cell evoked by 10 mV step commands from -60 to -140 mV. Scale bars, 150 pA, 200 ms. *B*, *I–V* relationship of currents sensitive to 40 μM Ba^{2+} as in *A*. Note strong increase of inwardly rectifying component in epileptic granule cells. Inset, the Ba^{2+}-insensitive currents lacked inward rectification and were also increased in epileptic granule cells. Scale bars, 50 pA, 10 mV. *C*, inhibition of inward currents (evoked at -120 mV) by Ba^{2+} revealed that a major component of these currents displays a high Ba^{2+} sensitivity. $IC_{50} \pm$ S.D. values, Hill coefficients and relative base levels were $14.3 \pm 2.5 \mu$M, -1.22 and 0.26 for control ($n = 37$) and $19.2 \pm 2.3 \mu$M, -1.37 and 0.19 for epileptic cells ($n = 34$), respectively. *D*, the Ba^{2+} sensitivity of inward currents was decreased towards more physiological potentials as has been described for Kir2 channels (see text). Values in bars are numbers of cells.
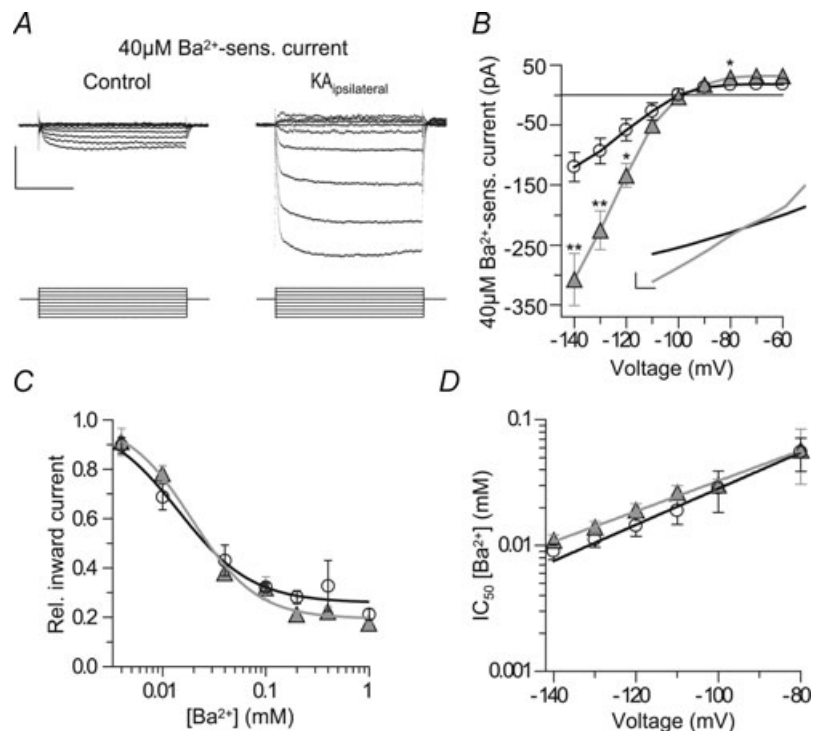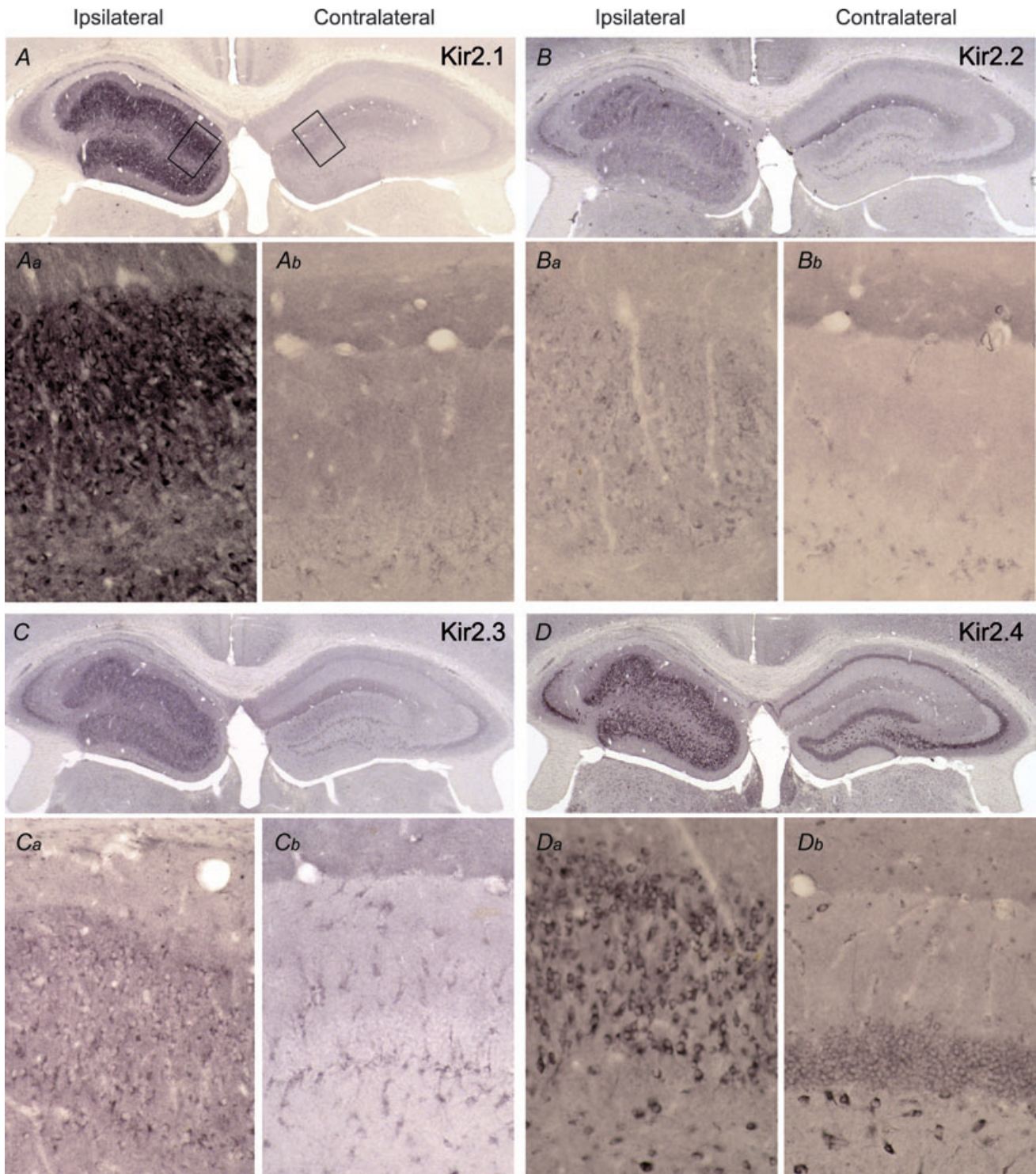
Figure 7. Kir2 channel proteins are elevated in epileptic granule cells
Staining of Kir2 (Kir2.1–Kir2.4) family proteins was strongly increased in the epileptic as compared to the contralateral dentate gyrus (*A*, *B*, *C*, *D*, left *vs.* right hippocampus). At higher magnification (see boxed areas in *A*) elevated Kir2.1 expression was detected primarily in somata of epileptic (*Aa*) *vs.* contralateral (*Ab*) granule cells. Expression of Kir2.2 (*B*, *Ba*) and Kir2.3 (*C*, *Ca*) proteins was also elevated in the injected hippocampus. Kir2.4 subunit protein was more strongly expressed in the injected hippocampus (*D*, *Da*) as compared to the contralateral side (*Db*) and still more to that of the Kir2.2 and Kir2.3 proteins. Note the elevated level of the Kir2.4 protein in subareas of the CA3 field (*D*; compare to Fig. 1*A* and *B*).

immunoperoxidase reaction is not feasible, the increase in the case of Kir2.1 subunits appeared particularly strong (Fig. 7*A*). As the granule cell density is lower on the injected side, this is a conservative estimate. At higher magnification the increased Kir2 labelling on the epileptic side could be attributed to an intense cytoplasmatic labelling of granule cells (Fig. 7, compare *Aa* with *Ab*, *Ba* with *Bb*, *Ca* with *Cb* and *Da* with *Db*, respectively). Interestingly, in the CA3a and CA3b subareas, where pyramidal cells survived epilepsy (Fig. 1*A* arrow, *B*), Kir2.2, Kir2.3, and especially Kir2.4 channel proteins also appeared upregulated (Fig. 7*B*–*D*).

In summary, consistent with our electrophysiological results, the expression of Kir2 channels was substantially enhanced in epileptic granule cells suggesting that it was responsible for the increased Kir currents of epileptic granule cells in TLE.

Twik channel proteins are elevated in epileptic granule cells

Our electrophysiological data indicated that part of the increased conductance of epileptic granule cells may have been mediated by non-rectifying or weakly rectifying K^+ channels such as the two-pore K^+ (K2P) channels of the Twik1/K2P1.1 or Twik2/K2P6.1 subtype (Goldstein *et al.* 2001; Patel & Honore, 2001). Indeed, the immunocytochemical staining for the Twik1 channel protein showed a striking upregulation on the KA-lesioned side (Fig. 8*A*, *Aa* and *Ab*). However, whether this strong accumulation of Twik1 proteins is paralleled by an elevated Twik1 channel level in the plasma membrane cannot be deduced from our morphological data. The immunoreactivity for Twik1 did not allow localization of the protein at the cellular level, but as granule cells are the main
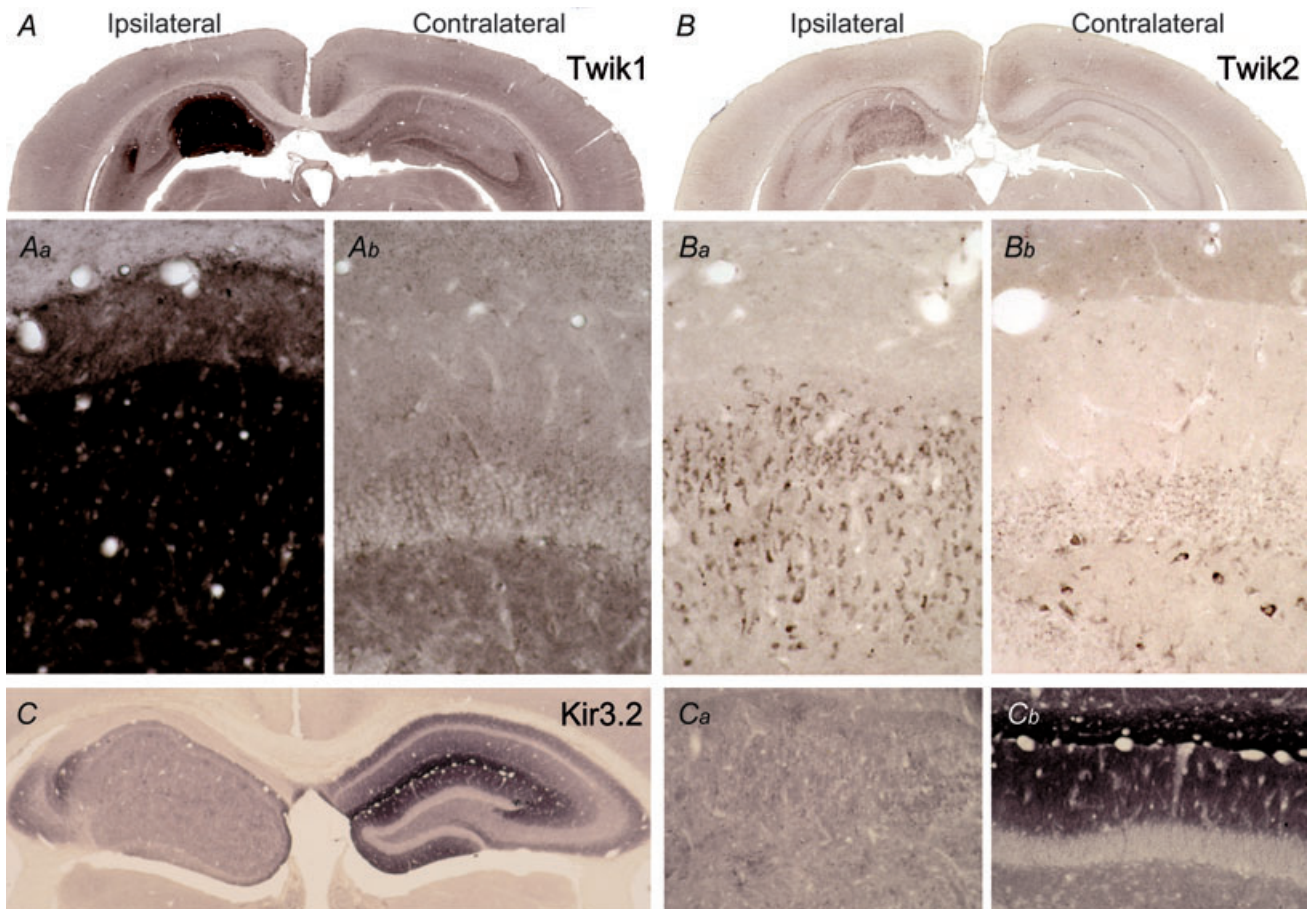

Figure 8. Twik channel proteins are elevated in epileptic granule cells
Expression of Twik1 protein is strongly increased in the KA-injected hippocampus (*A*, *Aa*) compared to the contralateral side (*A*, *Ab*) but staining is too intense to differentiate somatic from dendritic channel distribution. Note the strong Twik1 immunoreactivity in the molecular layer of the epileptic dentate gyrus, which via three capillaries is demarcated from the stratum lacunosum-moleculare above (*Aa*, see also Fig. 1*B*). Expression of Twik2 protein is also slightly increased in the injected hippocampus (*B*, *Ba*). In contrast, levels of Kir3.2 proteins are decreased in the ipsilateral hippocampus (*C*, *Ca*, *Cb*).

surviving cells in this area it is likely that Twik1 expression was enhanced in granule cells. Possibly it was elevated in other cell types (e.g. glial cells) in addition. Twik2 channels were clearly expressed in granule cells although their main expression sites have been reported to be outside the CNS (Medhurst *et al.* 2001). Also, the Twik2 immunoreactivity was increased in epileptic granule cells albeit to a smaller extent (Fig. 8*B*, *Ba* and *Bb*).

Although our pharmacological evidence argued against a contribution of Kir3.2 channels to the increased g_{rest} we wanted to verify whether Kir3.2 channels, presumably the predominant conducting subunit of G-protein-coupled Kir (Girk/Kir3) channels in granule cells (Karschin *et al.* 1996; Liao *et al.* 1996), showed elevated immunolabelling in the KA-injected hippocampus. However, neither the Kir3.2 protein (Fig. 8*C*), nor any of the other Kir3 channel proteins (data not shown) were elevated on the injected side. As expected (Liao *et al.* 1996), the Kir3.2 subunit displayed a highly laminar distribution in the contralateral hippocampus with highest densities in the stratum lacunosum-moleculare of the CA1 region and the molecular layer of the dentate gyrus (Fig. 8*C* and *Cb*). In contrast, Kir3.2 expression on the epileptic side was homogeneously low (Fig. 8*C* and *Ca*) and even at higher magnification rather down- than upregulated.

In summary, while the elevated Twik channel expression probably contributed to the increased g_{rest} and may contribute to leak components with less inward rectification and lower Ba^{2+} sensitivity, the enhanced expression of Kir2 channels explains the epilepsy-induced increase in Kir currents with high Ba^{2+} sensitivity in epileptic granule cells.

Discussion

The main finding reported here is that the passive membrane properties of dentate gyrus granule cells are fundamentally altered in a TLE model with AHS and GCD. Previous work has suggested that granule cells become intrinsically hyperexcitable in TLE via changes in ion channels (Isokawa & Mello, 1991; Beck *et al.* 1998; Selke *et al.* 2006). The data presented here suggest that changes in the passive cellular properties related to the degree of AHS have to be taken into account in addition, to fully characterize the excitability of granule cells in TLE.

Epileptic (dispersed) granule cells of mice with intrahippocampal kainate injection display increased membrane conductivity and a decreased excitability

In the sclerotic focus of KA-injected mice, granule cells possessed a strongly reduced R_{in} and τ_m, both important factors in postsynaptic signal integration (Fig. 1). Indeed, much more current was needed to drive epileptic granule

cells to action potential firing (Fig. 2), suggesting their excitability was decreased rather than increased (our label 'epileptic' for ipsilateral cells should not be confounded with 'more excitable'). As previously observed, granule cells of KA-injected mice displayed an altered morphology (Suzuki *et al.* 1995, 1997) which we considered here only with respect to its impact on R_{in}. Our morphological quantifications of reconstructed cells and computer simulations show that the R_{in} difference between control and epileptic cells was not due to the increased soma surface or a changed cellular geometry (Fig. 3). Thus, the simultaneous decrease of R_{in} and τ_m is only compatible with the interpretation that the membrane conductivity ($1/R_m$) of epileptic granule cells was increased. No such decrease in R_{in} has been mentioned in any of the many earlier patch-clamp studies of granule cells using other TLE animal models (e.g. Mody *et al.* 1992; Isokawa, 1996*b*; Molnar & Nadler, 1999; Okazaki *et al.* 1999; Scharfman *et al.* 2000; Dietrich *et al.* 2005; but see Isokawa & Mello, 1991). This discrepancy could be related to the seizure extent and the degree of hippocampal damage. In many of the earlier TLE studies, models were used where CA pyramidal and granule cell layers appear to be less affected compared to the TLE model used here. In particular, very little GCD is observed in these rat TLE models (Okazaki *et al.* 1999; Scharfman *et al.* 2000; Dietrich *et al.* 2005). Interestingly, in one study a decrease in τ_m was reported which was associated with increased frequency of seizures, whereas with lower seizure frequency τ_m remained unchanged (Isokawa, 1996*a*).

We found a correlation of granule cell membrane conductivity and the degree of GCD in the present work (Fig. 1) and in TLE patients (Stegen *et al.* 2009). How could GCD and R_{in} be related? It has been shown that GCD is not a direct effect of the KA itself but rather a consequence of disturbed reelin signalling which also occurs in TLE (Haas *et al.* 2002; Suzuki *et al.* 2005; Heinrich *et al.* 2006). We cannot fully exclude that conductivity changes are triggered by the KA, but as they first occur several days after KA injection, this seems unlikely. In addition, similar effects occur in TLE patients (Stegen *et al.* 2009). Reeler mice share GCD mechanisms with TLE but lack hippocampal epilepsy. If GCD itself would directly cause the changed conductivity, one would expect to find a decreased R_{in} in granule cells of reeler mice. However, this is not the case (J. Kowalski, personal communication). The combined data favour the hypothesis that GCD and the leakiness of granule cells are two independent consequences of seizure activity which may vary in different forms of TLE (Mueller *et al.* 2007). This hypothesis implies that the morphological and physiological changes reported here are either delayed responses to the status epilepticus or a response to seizures occurring in the first 2 weeks after KA injection which has sometimes been called 'latent period' (but see Sloviter,

2008). Indeed, EEG recordings revealed that subclinical seizures are frequent in the first 2 weeks after intra-hippocampal KA injection (Bouilleret *et al.* 1999; Riban *et al.* 2002; U. Häussler, personal communication).

Epileptic granule cells possessed increased potassium and GABA$_A$ leak conductances

Our K$^+$ replacement experiments suggest that the increased leak conductance of epileptic granule cells was mainly ($\sim$70–80%) due to an increased K$^+$ conductance (Fig. 4). At V_{rest} roughly 50% of this increased K$^+$ conductance was sensitive to 1 mM Ba^{2+} while the remaining part was not. In addition, a ($\sim$20–30%) GABA$_A$ conductance contributed to the leak increased in epileptic granule cells (Fig. 5). These estimates of relative contributions should be treated with caution because they had to be calculated across cells and animals among which the variance was high. In individual experiments, the contributions to the leak ranged between almost equal BMI-sensitive and (200 μM) Ba^{2+}-sensitive g_{rest}, respectively, in one cell and only $\sim$5% GABA$_A$ and $\sim$95% highly Ba^{2+}-sensitive leak in other cells. The increased GABA$_A$ conductance of epileptic granule cells could explain why these cells were not hyperpolarized despite the increase in K$^+$ conductance as the reversal potential of GABA$_A$ currents was depolarizing in our conditions (see also Staley & Mody, 1992; Soltesz & Mody, 1994). In the context of excitability, it should be stressed that the slight depolarization ($\sim$3 mV) of epileptic granule cells was largely overruled by the reduction in R_{in}. This is evident from the rheobase which was tripled in epileptic cells.

So-called tonic GABA$_A$ currents, which generally can only be revealed in granule cells by pharmacological manipulations, constitute a good candidate for the GABA$_A$-mediated leak conductance we found (Stell *et al.* 2003; Farrant & Nusser, 2005; Glykys *et al.* 2008). In granule cells, tonic currents are thought to be mediated by extrasynaptic GABA$_A$ receptors likely to contain δ subunits associated to α5 and/or α4 subunits (Peng *et al.* 2002; Stell *et al.* 2003; Farrant & Nusser, 2005; Glykys *et al.* 2008). The expression of α5 and α4 subunits has indeed been found upregulated in TLE although not in all cases (Schwarzer *et al.* 1997; Brooks-Kayal *et al.* 1998; Loup *et al.* 2000; Peng *et al.* 2004; Sun *et al.* 2007; Zhang *et al.* 2007). In most of these studies, the expression of δ subunits appeared downregulated but other subunits usually not mediating tonic currents may compensate for this loss (Nusser *et al.* 1998; Peng *et al.* 2002; Sun *et al.* 2007; Zhang *et al.* 2007). Importantly, in the TLE model we used, α5 expression is increased in the dentate gyrus (Bouilleret *et al.* 2000). Thus, it is likely that we measured the functional correlate of the GABA$_A$ receptor upregulation in TLE. As the competitive GABA$_A$ antagonist BMI had almost the same effect on g_{rest} as the non-competitive chloride channel blocker PTX, our results suggest that most of the GABAergic leak was mediated by receptor activation rather than constitutive opening of GABA$_A$ receptors independent of agonist binding.

Our results suggest that inwardly rectifying K$^+$ (Kir) channels mediated the Ba^{2+}-sensitive component of the increased g_{rest} (see below). However, another K$^+$ conductance with lower Ba^{2+} sensitivity ($>$ 2 mM) and less rectification (Fig. 6B) appeared to contribute to the leak of epileptic granule cells (see 32% residual g_{rest} fitted to the dose–response data in Fig. 5D). These properties are compatible with two-pore leak K$^+$ (K2P) channels such as weak inward rectifier K$^+$ (Twik) channels (Goldstein *et al.* 2001; Patel & Honore, 2001). Indeed, we found a marked upregulation of Twik1/K2P1.1 channels and a weak increase of Twik2/K2P6.1 channels on the KA-injected side, suggesting Twik channels also contributed to the increased leak. However, because the Ba^{2+} sensitivity of Twik channels under physiological conditions is not entirely clear (Goldstein *et al.* 2001; Patel & Honore, 2001) we cannot conclude with certainty about the contribution of Twik channels. Less Ba^{2+}-sensitive K2P channels such as Twik-related acid-sensitive K2P (Task) channels have now also been reported as increased in the pilocarpine model of TLE (Kim *et al.* 2009) although it is unclear how this relates to the lack of R_{in} changes reported repeatedly from the same model (see above). In the TLE model used here, we could not find an increased sensitivity of the pathological g_{rest} to lowered pH. Other ion channels affected in TLE include HCN channels (Bender *et al.* 2003) and the effectors of GABA$_B$ receptors (Kir3/Girk channels) (Straessle *et al.* 2003). However, our pharmacological experiments gave no evidence that any of these channels (and Kv channels or calcium-activated K$^+$ channels) contributed to the g_{rest} of epileptic granule cells. Also, increased NMDA receptor activation could contribute to a decreased R_{in} in TLE (Isokawa & Mello, 1991), but in our TLE model inhibition of glutamate receptors did not affect the g_{rest} of epileptic granule cells.

Kir2 channels are responsible for the increased inwardly rectifying K$^+$ currents of epileptic granule cells

In epileptic granule cells, highly Ba^{2+}-sensitive currents (IC$_{50}$: $\sim$19 μM at -120 mV and physiological K$^+$) with marked inward rectification were strongly increased (Fig. 6). These properties match the profile of classical inward rectifier K$^+$ (Irk1–4/Kir2.1–2.4) channels (Goldstein *et al.* 2001; Preisig-Muller *et al.* 2002; Schram *et al.* 2002; Kubo *et al.* 2005), but are incompatible with the properties of weak inward or even outward rectifier

K$^+$ channels (Coetzee *et al.* 1999; Goldstein *et al.* 2001; Liu *et al.* 2001; Patel & Honore, 2001). Consistent with this interpretation, we found a robust upregulation of Kir2 channel protein in epileptic compared to contralateral granule cells. Although the increase in immunoreactivity appeared most prominent for Kir2.1 and Kir2.4 subunits, our data do not allow a determination of a differential contribution of subunits Kir2.1–2.4 which form heteromultimers with intermediate pharmacological properties (Preisig-Muller *et al.* 2002; Schram *et al.* 2002).

Kir2 channels are also important for K$^+$ buffering mediated by astrocytes but this capacity seems to be rather decreased in the epileptic hippocampus (Bordey & Sontheimer, 1998; Jabs *et al.* 2008). Interestingly, an upregulation of Kir2.1 channels in glial cells has been observed in the acute phase after systemic KA injection in mice (Kang *et al.* 2008). However, this study stated that in the dentate gyrus an increase of Kir2.1 channel-expressing cells was not prominent after KA injection and that most neurons failed to show Kir2.1 immunoreactivity. In contrast, the Kir2 antibodies used here clearly label neurons in the dentate gyrus (Pruss *et al.* 2005), consistent with other reports of Kir2 distribution (Karschin *et al.* 1996; Liao *et al.* 1996), and this labelling was increased after KA injection. Inward rectification has been previously observed in dentate granule cells (Zhang *et al.* 1993) although in dissociated granule cells of TLE patients it was not measured (Beck *et al.* 1996). Consistent with a role as 'resting channels' in other cell types (Goldstein *et al.* 2001; Stanfield *et al.* 2002; Kubo *et al.* 2005), our results suggest that Kir2 channels do control the V_{rest} and the R_{in} of granule cells and that these channels are strongly upregulated in TLE. Interestingly, a parallel study concluded that Kir2.1 channels control the excitability of granule cells (Mongiat *et al.* 2009).

In summary, we have shown that granule cells become 'leaky' with increasing severity of hippocampal sclerosis during experimental TLE. The membrane conductivity for K$^+$ ions was determined as the main reason for this leakiness, but a GABA$_A$-mediated conductance also contributed. At least half of the increased K$^+$ conductance was due to Kir2 channels, as highly Ba^{2+}-sensitive Kir2 currents and Kir2 protein expression was strongly increased in epileptic granule cells. In addition, a Ba^{2+}-insensitive K$^+$ conductance was involved which could not be identified, but may be due to the increased Twik channel expression. Leakiness is a property suitable to sustain high firing frequencies but also to shunt synaptic input and thereby to balance neuronal excitability. Thus, neurons in the sclerotic focus appear to acquire anti-convulsive properties. Indeed, most TLE seizures appear to be generated outside the area of greatest hippocampal damage (King *et al.* 1997; Le Duigou *et al.* 2008). Therefore we propose that the upregulation of leak conductances in granule cells constitutes an adaptive mechanism to partially counterbalance hyperexcitability in epilepsy.

References

Beck H, Blumcke I, Kral T, Clusmann H, Schramm J, Wiestler OD, Heinemann U & Elger CE (1996). Properties of a delayed rectifier potassium current in dentate granule cells isolated from the hippocampus of patients with chronic temporal lobe epilepsy. *Epilepsia* **37**, 892–901.

Beck H, Steffens R, Elger CE & Heinemann U (1998). Voltage-dependent Ca^{2+} currents in epilepsy. *Epilepsy Res* **32**, 321–332.

Bender RA, Soleymani SV, Brewster AL, Nguyen ST, Beck H, Mathern GW & Baram TZ (2003). Enhanced expression of a specific hyperpolarization-activated cyclic nucleotide-gated cation channel (HCN) in surviving dentate gyrus granule cells of human and experimental epileptic hippocampus. *J Neurosci* **23**, 6826–6836.

Blumcke I, Thom M & Wiestler OD (2002). Ammon's horn sclerosis: a maldevelopmental disorder associated with temporal lobe epilepsy. *Brain Pathol* **12**, 199–211.

Bordey A & Sontheimer H (1998). Properties of human glial cells associated with epileptic seizure foci. *Epilepsy Res* **32**, 286–303.

Bouilleret V, Loup F, Kiener T, Marescaux C & Fritschy JM (2000). Early loss of interneurons and delayed subunit-specific changes in GABA$_A$-receptor expression in a mouse model of mesial temporal lobe epilepsy. *Hippocampus* **10**, 305–324.

Bouilleret V, Ridoux V, Depaulis A, Marescaux C, Nehlig A & Le Gal La Salle G (1999). Recurrent seizures and hippocampal sclerosis following intrahippocampal kainate injection in adult mice: electroencephalography, histopathology and synaptic reorganization similar to mesial temporal lobe epilepsy. *Neuroscience* **89**, 717–729.

Brauer AU, Savaskan NE, Kole MH, Plaschke M, Monteggia LM, Nestler EJ, Simburger E, Deisz RA, Ninnemann O & Nitsch R (2001). Molecular and functional analysis of hyperpolarization-activated pacemaker channels in the hippocampus after entorhinal cortex lesion. *FASEB J* **15**, 2689–2701.

Brooks-Kayal AR, Shumate MD, Jin H, Rikhter TY & Coulter DA (1998). Selective changes in single cell GABA$_A$ receptor subunit expression and function in temporal lobe epilepsy. *Nat Med* **4**, 1166–1172.

Carnevale NT & Hines ML (2006). *The Neuron Book*. Cambridge University Press, Cambridge, UK.

Coetzee WA, Amarillo Y, Chiu J, Chow A, Lau D, McCormack T, Moreno H, Nadal MS, Ozaita A, Pountney D, Saganich M, Vega-Saenz de Miera E & Rudy B (1999). Molecular diversity of K$^+$ channels. *Ann N Y Acad Sci* **868**, 233–285.

Dietrich D, Podlogar M, Ortmanns G, Clusmann H & Kral T (2005). Calbindin-D28k content and firing pattern of hippocampal granule cells in amygdala-kindled rats: a perforated patch-clamp study. *Brain Res* **1032**, 123–130.

Eulitz D, Pruss H, Derst C & Veh RW (2007). Heterogeneous distribution of kir3 potassium channel proteins within dopaminergic neurons in the mesencephalon of the rat brain. *Cell Mol Neurobiol* **27**, 285–302.

Farrant M & Nusser Z (2005). Variations on an inhibitory theme: phasic and tonic activation of GABA$_A$ receptors. *Nat Rev Neurosci* **6**, 215–229.

Glykys J, Mann EO & Mody I (2008). Which GABA$_A$ receptor subunits are necessary for tonic inhibition in the hippocampus? *J Neurosci* **28**, 1421–1426.

Goldstein SA, Bockenhauer D, O'Kelly I & Zilberberg N (2001). Potassium leak channels and the KCNK family of two-P-domain subunits. *Nat Rev Neurosci* **2**, 175–184.

Haas CA, Dudeck O, Kirsch M, Huszka C, Kann G, Pollak S, Zentner J & Frotscher M (2002). Role for reelin in the development of granule cell dispersion in temporal lobe epilepsy. *J Neurosci* **22**, 5797–5802.

Hama K, Arii T & Kosaka T (1989). Three-dimensional morphometrical study of dendritic spines of the granule cell in the rat dentate gyrus with HVEM stereo images. *J Electron Microsc Tech* **12**, 80–87.

Harvey BD & Sloviter RS (2005). Hippocampal granule cell activity and c-Fos expression during spontaneous seizures in awake, chronically epileptic, pilocarpine-treated rats: implications for hippocampal epileptogenesis. *J Comp Neurol* **488**, 442–463.

Heinemann U, Beck H, Dreier JP, Ficker E, Stabel J & Zhang CL (1992). The dentate gyrus as a regulated gate for the propagation of epileptiform activity. *Epilepsy Res Suppl* **7**, 273–280.

Heinrich C, Nitta N, Flubacher A, Muller M, Fahrner A, Kirsch M, Freiman T, Suzuki F, Depaulis A, Frotscher M & Haas CA (2006). Reelin deficiency and displacement of mature neurons, but not neurogenesis, underlie the formation of granule cell dispersion in the epileptic hippocampus. *J Neurosci* **26**, 4701–4713.

Houser CR (1990). Granule cell dispersion in the dentate gyrus of humans with temporal lobe epilepsy. *Brain Res* **535**, 195–204.

Isokawa M (1996*a*). Decreased time constant in hippocampal dentate granule cells in pilocarpine-treated rats with progressive seizure frequencies. *Brain Res* **718**, 169–175.

Isokawa M (1996*b*). Decrement of GABA$_A$ receptor-mediated inhibitory postsynaptic currents in dentate granule cells in epileptic hippocampus. *J Neurophysiol* **75**, 1901–1908.

Isokawa M & Mello LE (1991). NMDA receptor-mediated excitability in dendritically deformed dentate granule cells in pilocarpine-treated rats. *Neurosci Lett* **129**, 69–73.

Jabs R, Seifert G & Steinhauser C (2008). Astrocytic function and its alteration in the epileptic brain. *Epilepsia* **49**, 3–12.

Kang SJ, Cho SH, Park K, Yi J, Yoo SJ & Shin KS (2008). Expression of kir2.1 channels in astrocytes under pathophysiological conditions. *Mol Cells* **25**, 124–130.

Karschin C, Dissmann E, Stuhmer W & Karschin A (1996). IRK(1–3) and GIRK(1–4) inwardly rectifying K$^+$ channel mRNAs are differentially expressed in the adult rat brain. *J Neurosci* **16**, 3559–3570.

Kim JE, Kwak SE & Kang TC (2009). Upregulated TWIK-related acid-sensitive K$^+$ channel-2 in neurons and perivascular astrocytes in the hippocampus of experimental temporal lobe epilepsy. *Epilepsia* **50**, 654–663.

King D, Bronen RA, Spencer DD & Spencer SS (1997). Topographic distribution of seizure onset and hippocampal atrophy: relationship between MRI and depth EEG. *Electroencephalogr Clin Neurophysiol* **103**, 692–697.

Kralic JE, Ledergerber DA & Fritschy JM (2005). Disruption of the neurogenic potential of the dentate gyrus in a mouse model of temporal lobe epilepsy with focal seizures. *Eur J Neurosci* **22**, 1916–1927.

Kubo Y, Adelman JP, Clapham DE, Jan LY, Karschin A, Kurachi Y, Lazdunski M, Nichols CG, Seino S & Vandenberg CA (2005). International Union of Pharmacology. LIV. Nomenclature and molecular relationships of inwardly rectifying potassium channels. *Pharmacol Rev* **57**, 509–526.

Le Duigou C, Bouilleret V & Miles R (2008). Epileptiform activities in slices of hippocampus from mice after intra-hippocampal injection of kainic acid. *J Physiol* **586**, 4891–4904.

Le Duigou C, Wittner L, Danglot L & Miles R (2005). Effects of focal injection of kainic acid into the mouse hippocampus *in vitro* and *ex vivo*. *J Physiol* **569**, 833–847.

Liao YJ, Jan YN & Jan LY (1996). Heteromultimerization of G-protein-gated inwardly rectifying K$^+$ channel proteins GIRK1 and GIRK2 and their altered expression in weaver brain. *J Neurosci* **16**, 7137–7150.

Liu GX, Derst C, Schlichthorl G, Heinen S, Seebohm G, Bruggemann A, Kummer W, Veh RW, Daut J & Preisig-Muller R (2001). Comparison of cloned Kir2 channels with native inward rectifier K$^+$ channels from guinea-pig cardiomyocytes. *J Physiol* **532**, 115–126.

Liu M, Pleasure SJ, Collins AE, Noebels JL, Naya FJ, Tsai MJ & Lowenstein DH (2000). Loss of BETA2/NeuroD leads to malformation of the dentate gyrus and epilepsy. *Proc Natl Acad Sci U S A* **97**, 865–870.

Loup F, Wieser HG, Yonekawa Y, Aguzzi A & Fritschy JM (2000). Selective alterations in GABAA receptor subtypes in human temporal lobe epilepsy. *J Neurosci* **20**, 5401–5419.

Medhurst AD, Rennie G, Chapman CG, Meadows H, Duckworth MD, Kelsell RE, Gloger II & Pangalos MN (2001). Distribution analysis of human two pore domain potassium channels in tissues of the central nervous system and periphery. *Brain Res Mol Brain Res* **86**, 101–114.

Mody I, Kohr G, Otis TS & Staley KJ (1992). The electrophysiology of dentate gyrus granule cells in whole-cell recordings. *Epilepsy Res Suppl* **7**, 159–168.

Mody I, Stanton PK & Heinemann U (1988). Activation of N-methyl-D-aspartate receptors parallels changes in cellular and synaptic properties of dentate gyrus granule cells after kindling. *J Neurophysiol* **59**, 1033–1054.

Molnar P & Nadler JV (1999). Mossy fiber-granule cell synapses in the normal and epileptic rat dentate gyrus studied with minimal laser photostimulation. *J Neurophysiol* **82**, 1883–1894.

Mongiat LA, Esposito MS, Lombardi G & Schinder AF (2009). Reliable activation of immature neurons in the adult hippocampus. *PLoS ONE* **4**, e5320.

Mueller SG, Laxer KD, Schuff N & Weiner MW (2007). Voxel-based T2 relaxation rate measurements in temporal lobe epilepsy (TLE) with and without mesial temporal sclerosis. *Epilepsia* **48**, 220–228.

Nusser Z, Hajos N, Somogyi P & Mody I (1998). Increased number of synaptic GABA$_A$ receptors underlies potentiation at hippocampal inhibitory synapses. *Nature* **395**, 172–177.

Okazaki MM, Molnar P & Nadler JV (1999). Recurrent mossy fiber pathway in rat dentate gyrus: synaptic currents evoked in presence and absence of seizure-induced growth. *J Neurophysiol* **81**, 1645–1660.

Patel AJ & Honore E (2001). Properties and modulation of mammalian 2P domain K$^+$ channels. *Trends Neurosci* **24**, 339–346.

Peng Z, Hauer B, Mihalek RM, Homanics GE, Sieghart W, Olsen RW & Houser CR (2002). GABA$_A$ receptor changes in delta subunit-deficient mice: altered expression of α4 and γ2 subunits in the forebrain. *J Comp Neurol* **446**, 179–197.

Peng Z, Huang CS, Stell BM, Mody I & Houser CR (2004). Altered expression of the delta subunit of the GABA$_A$ receptor in a mouse model of temporal lobe epilepsy. *J Neurosci* **24**, 8629–8639.

Preisig-Muller R, Schlichthorl G, Goerge T, Heinen S, Bruggemann A, Rajan S, Derst C, Veh RW & Daut J (2002). Heteromerization of Kir2.x potassium channels contributes to the phenotype of Andersen's syndrome. *Proc Natl Acad Sci U S A* **99**, 7774–7779.

Pruss H, Derst C, Lommel R & Veh RW (2005). Differential distribution of individual subunits of strongly inwardly rectifying potassium channels (Kir2 family) in rat brain. *Brain Res Mol Brain Res* **139**, 63–79.

Pruss H, Wenzel M, Eulitz D, Thomzig A, Karschin A & Veh RW (2003). Kir2 potassium channels in rat striatum are strategically localized to control basal ganglia function. *Brain Res Mol Brain Res* **110**, 203–219.

Riban V, Bouilleret V, Pham-Le BT, Fritschy JM, Marescaux C & Depaulis A (2002). Evolution of hippocampal epileptic activity during the development of hippocampal sclerosis in a mouse model of temporal lobe epilepsy. *Neuroscience* **112**, 101–111.

Scharfman HE, Goodman JH & Sollas AL (2000). Granule-like neurons at the hilar/CA3 border after status epilepticus and their synchrony with area CA3 pyramidal cells: functional implications of seizure-induced neurogenesis. *J Neurosci* **20**, 6144–6158.

Schmidt-Hieber C, Jonas P & Bischofberger J (2004). Enhanced synaptic plasticity in newly generated granule cells of the adult hippocampus. *Nature* **429**, 184–187.

Schmidt-Hieber C, Jonas P & Bischofberger J (2007). Subthreshold dendritic signal processing and coincidence detection in dentate gyrus granule cells. *J Neurosci* **27**, 8430–8441.

Schram G, Melnyk P, Pourrier M, Wang Z & Nattel S (2002). Kir2.4 and Kir2.1 K$^+$ channel subunits co-assemble: a potential new contributor to inward rectifier current heterogeneity. *J Physiol* **544**, 337–349.

Schwarzer C, Tsunashima K, Wanzenbock C, Fuchs K, Sieghart W & Sperk G (1997). GABA$_A$ receptor subunits in the rat hippocampus II: altered distribution in kainic acid-induced temporal lobe epilepsy. *Neuroscience* **80**, 1001–1017.

Selke K, Muller A, Kukley M, Schramm J & Dietrich D (2006). Firing pattern and calbindin-D28k content of human epileptic granule cells. *Brain Res* **1120**, 191–201.

Sloviter RS (1991). Permanently altered hippocampal structure, excitability, and inhibition after experimental status epilepticus in the rat: the 'dormant basket cell' hypothesis and its possible relevance to temporal lobe epilepsy. *Hippocampus* **1**, 41–66.

Sloviter RS (1994). The functional organization of the hippocampal dentate gyrus and its relevance to the pathogenesis of temporal lobe epilepsy. *Ann Neurol* **35**, 640–654.

Sloviter RS (2008). Hippocampal epileptogenesis in animal models of mesial temporal lobe epilepsy with hippocampal sclerosis: the importance of the 'latent period' and other concepts. *Epilepsia* **49**, 85–92.

Soltesz I & Mody I (1994). Patch-clamp recordings reveal powerful GABAergic inhibition in dentate hilar neurons. *J Neurosci* **14**, 2365–2376.

Staley KJ & Mody I (1992). Shunting of excitatory input to dentate gyrus granule cells by a depolarizing GABA$_A$ receptor-mediated postsynaptic conductance. *J Neurophysiol* **68**, 197–212.

Stanfield PR, Nakajima S & Nakajima Y (2002). Constitutively active and G-protein coupled inward rectifier K$^+$ channels: Kir2.0 and Kir3.0. *Rev Physiol Biochem Pharmacol* **145**, 47–179.

Stegen M, Young CC, Haas CA, Zentner J & Wolfart J (2009). Increased leak conductance in dentate gyrus granule cells of temporal lobe epilepsy patients with Ammon's horn sclerosis. *Epilepsia* **50**, 646–653.

Stell BM, Brickley SG, Tang CY, Farrant M & Mody I (2003). Neuroactive steroids reduce neuronal excitability by selectively enhancing tonic inhibition mediated by δ subunit-containing GABA$_A$ receptors. *Proc Natl Acad Sci U S A* **100**, 14439–14444.

Straessle A, Loup F, Arabadzisz D, Ohning GV & Fritschy JM (2003). Rapid and long-term alterations of hippocampal GABA$_B$ receptors in a mouse model of temporal lobe epilepsy. *Eur J Neurosci* **18**, 2213–2226.

Sun C, Mtchedlishvili Z, Erisir A & Kapur J (2007). Diminished neurosteroid sensitivity of synaptic inhibition and altered location of the α4 subunit of GABA$_A$ receptors in an animal model of epilepsy. *J Neurosci* **27**, 12641–12650.

Suzuki F, Heinrich C, Boehrer A, Mitsuya K, Kurokawa K, Matsuda M & Depaulis A (2005). Glutamate receptor antagonists and benzodiazepine inhibit the progression of granule cell dispersion in a mouse model of mesial temporal lobe epilepsy. *Epilepsia* **46**, 193–202.

Suzuki F, Junier MP, Guilhem D, Sorensen JC & Onteniente B (1995). Morphogenetic effect of kainate on adult hippocampal neurons associated with a prolonged expression of brain-derived neurotrophic factor. *Neuroscience* **64**, 665–674.

Suzuki F, Makiura Y, Guilhem D, Sorensen JC & Onteniente B (1997). Correlated axonal sprouting and dendritic spine formation during kainate-induced neuronal morphogenesis in the dentate gyrus of adult mice. *Exp Neurol* **145**, 203–213.

Thom M, Sisodiya SM, Beckett A, Martinian L, Lin WR, Harkness W, Mitchell TN, Craig J, Duncan J & Scaravilli F (2002). Cytoarchitectural abnormalities in hippocampal sclerosis. *J Neuropathol Exp Neurol* **61**, 510–519.

Williamson A, Telfeian AE & Spencer DD (1995). Prolonged GABA responses in dentate granule cells in slices isolated from patients with temporal lobe sclerosis. *J Neurophysiol* **74**, 378–387.

Zhang L, Valiante TA & Carlen PL (1993). Contribution of the low-threshold T-type calcium current in generating the post-spike depolarizing afterpotential in dentate granule neurons of immature rats. *J Neurophysiol* **70**, 223–231.

Zhang N, Wei W, Mody I & Houser CR (2007). Altered localization of GABA$_A$ receptor subunits on dentate granule cell dendrites influences tonic and phasic inhibition in a mouse model of epilepsy. *J Neurosci* **27**, 7520–7531.

Author contributions

C.C. Young: Completion and analysis of electrophysiological experiments. Completion and analysis of morphological quantifications and Neurolucida analysis. Analysis of immuno-cytochemical experiments (Fig. 1*C*). Critical revision of manuscript. M. Stegen: Surgical procedures of KA injections. Completion and analysis of electrophysiological experiments. Computation of cable models. Critical revision of manuscript. R. Bernard: Completion of immunocytochemical experiments (Figs 1*A*, *B*, 7 and 8). Critical revision of manuscript. M. Müller: Surgical procedures of KA injections. Critical revision of manuscript. J. Bischofberger: Supervision and completion of confocal reconstructions. Critical revision of manuscript. R.W. Veh: Supervision and analysis of immuno-cytochemical experiments (Figs 1*A*, *B*, 7 and 8). Critical revision of manuscript. C.A. Haas: Conception of study. Critical revision of manuscript. J. Wolfart: Conception, design and supervision of study. Design and supervision of electrophysiological experiments. Conception of immuno-histochemical and morphological experiments. Drafting the manuscript.